medRxiv preprint doi: https://doi.org/10.1101/2020.05.07.20093963.this version posted May 11, 2020. The copyright holder for this preprint (which was not certified by peer review) is the author/funder, who has granted medRxiv a license to display the preprint in perpetuity. It is made available under a CC-BY-NC-ND 4.0 International license .

# Serological signatures of SARS-CoV-2 infection: Implications for antibody-based diagnostics

Jason ROSADO[1], Charlotte COCKRAM[2], Sarah Hélène MERKLING[3], Caroline DEMERET[4], Annalisa MEOLA[5], Solen KERNEIS[6,7], Benjamin TERRIER[8,9], Samira FAFI-KREMER[10,11], Jerome de SEZE[12], Marija BACKOVIC[5], Ivo MUELLER[1,13], Michael WHITE[1]*

1. Malaria: Parasites and Hosts Unit, Department of Parasites and Insect Vectors, Institut Pasteur, Paris, France
2. Spatial Regulation of Genomes Unit, Department of Genomes and Genetics, Institut Pasteur, Paris, France
3. Insect-Virus Interactions Unit, Department of Virology, Institut Pasteur, Paris, France
4. Molecular Genetics of RNA Viruses Unit, Department of Virology, Institut Pasteur, Paris, France
5. Structural Virology Unit, Department of Virology and CNRS UMR 3569, Institut Pasteur, Paris, France
6. Equipe Mobile d'Infectiologie, APHP Centre-Université de Paris, Paris, France
7. Epidemiology and Modelling of Bacterial Escape to Antimicrobials Unit, Department of Global Health, Institut Pasteur, Paris, France
8. Department of Internal Medicine, National Referral Center for Rare Systemic Autoimmune Diseases, Assistance Publique Hôpitaux de Paris-Centre (APHP-CUP), Université de Paris, Paris, France
9. PARCC, INSERM U970, Paris, France
10. CHU de Strasbourg, Laboratoire de Virologie, F-67091 Strasbourg, France
11. Université de Strasbourg, INSERM, IRM UMR_S 1109, Strasbourg, France
12. Centre d'Investigation Clinique - INSERM CIC-1434, Strasbourg, France
13. Division of Population Health and Immunity, The Walter and Eliza Hall Institute, Melbourne, Australia

***Correspondence**

Dr Michael White

Malaria: Parasites and Hosts Unit
Department of Parasites and Insect Vectors
Institut Pasteur
25-28 Rue du Docteur Roux
Paris 75015
France

e-mail: michael.white@pasteur.fr

Prof Ivo Mueller

Division of Population Health and Immunity
The Walter and Eliza Hall Institute of Medical Research
1G Royal Parade
Parkville
Victoria 3052
Australia

e-mail: mueller@wehi.edu.au

medRxiv preprint doi: https://doi.org/10.1101/2020.05.07.20093963.this version posted May 11, 2020. The copyright holder for this preprint (which was not certified by peer review) is the author/funder, who has granted medRxiv a license to display the preprint in perpetuity. It is made available under a CC-BY-NC-ND 4.0 International license .


# Abstract

**Background**

The antibody response generated following infection with SARS-CoV-2 is expected to decline over time. This may cause individuals with confirmed SARS-CoV-2 infection to test negative according to serological diagnostic tests in the months and years following symptom onset.

**Methods**

A multiplex serological assay was developed to measure IgG and IgM antibody responses to four SARS-CoV-2 Spike (S) antigens: spike trimeric ectodomain ($S^{tri}$), its receptor-binding domain (RBD), spike subunit 1 (S1), and spike subunit 2 (S2). Antibody responses were measured in serum samples from patients in French hospitals with RT-qPCR confirmed infection (*n* = 259), and negative control serum samples collected before the start of the SARS-CoV-2 epidemic in 2019 (*n* = 335). The multiplex antibody data was used to train a random forests algorithm for classifying individuals with previous SARS-CoV-2 infection. A mathematical model of antibody kinetics informed by prior information from other coronaviruses was used to estimate time-varying antibody responses and assess the potential sensitivity and classification performance of serological diagnostics during the first year following symptom onset.

**Results**

IgG antibody responses to one S antigen identified individuals with previous RT-qPCR confirmed SARS-CoV-2 infection with 90.3% sensitivity (95% confidence interval (CI); 86.1%, 93.4%) and 99.1% specificity (95% CI; 97.4%, 99.7%). Using a serological signature of IgG to four antigens, it was possible to identify infected individuals with 96.1% sensitivity (95% CI; 93.0%, 97.9%) and 99.1% specificity (95% CI; 97.4%, 99.7%). Antibody responses to SARS-CoV-2 increase rapidly 1-2 weeks after symptom onset, with antibody responses predicted to peak within 2-4 weeks. Informed by prior data from other coronaviruses, one year following symptom onset antibody responses are predicted to decay by approximately 60% from the peak response. Depending on the selection of sero-positivity cutoff, we estimate that the sensitivity of serological diagnostics may reduce to 56% – 97% after six months, and to 49% – 93% after one year.

**Conclusion**

Serological signatures based on antibody responses to multiple antigens can provide more accurate and robust serological classification of individuals with previous SARS-CoV-2 infection. Changes in antibody levels over time may cause reductions in the sensitivity of serological diagnostics leading to an underestimation of sero-prevalence. It is essential that data continue to be collected to evaluate this potential risk.

medRxiv preprint doi: https://doi.org/10.1101/2020.05.07.20093963.this version posted May 11, 2020. The copyright holder for this preprint (which was not certified by peer review) is the author/funder, who has granted medRxiv a license to display the preprint in perpetuity. It is made available under a CC-BY-NC-ND 4.0 International license .

# Introduction

Severe acute respiratory syndrome coronavirus 2 (SARS-CoV-2) causing coronavirus disease 2019 (COVID-19) emerged in Wuhan, China in December 2019. Since then, it has spread rapidly, with confirmed cases being recorded in nearly every country in the world. The presence of viral infection can be directly detected via reverse transcriptase quantitative PCR (RT-qPCR) on samples from nasopharyngeal or throat swabs. For individuals who display symptoms, SARS-CoV-2 virus is detectable in the first 2-3 weeks following symptom onset [1,2]. Viral shedding is however shorter in mild cases with only upper respiratory tract symptoms (1-2 weeks) [3]. For asymptomatic individuals, the duration for which SARS-CoV-2 virus can be detected is uncertain. In most countries neither mild cases nor asymptomatic cases will be tested by RT-qPCR (unless they are direct contacts of known cases), and even among tested individuals many may be viremia negative at time of testing due to low viral load or improper sampling. While not suitable for diagnosis of clinical cases, serology is a promising tool for identifying individuals with previous infection by detecting antibodies generated in response to SARS-CoV-2. However, the utility of serological testing depends on the kinetics of the anti-SARS-CoV-2 antibody response during and after infection.

An individual is sero-positive to a pathogen if they have detectable antibodies specific for that pathogen. From an immunological perspective, an individual can be defined as sero-positive if they have either antibody secreting plasma cells and/or a matured memory B cell response to antigens on that pathogen. In practice, serological assays are used to measure antibody responses in blood samples. However, individuals who have never been infected with the target pathogen may have non-zero antibody responses due to cross-reactivity with other pathogens or background assay noise. To account for this, defining sero-positivity is reduced to determining whether the measured antibody responses is greater or lower than some defined cutoff value [4].

The most fundamental measure of antibody level is via concentration in a sample (e.g. in units of µg/mL), however a measurement in terms of molecular mass per volume is usually impossible to obtain. Instead, a range of assays can provide measurements that are positively associated with the true antibody concentration, e.g. an optical density from an enzyme-linked immunosorbent assay (ELISA), or a median fluorescent intensity (MFI) from a Luminex assay. In contrast to the continuous measurement of antibody response provided by laboratory-based research assays, most point-of-care serological tests provide a binary outcome: sero-negative or sero-positive. There are several commercially available tests for detecting SARS-CoV-2 antibody responses, which are being catalogued by FIND Diagnostics [5]. These tests are typically based on lateral flow assays mounted in plastic cartridges which detect antibodies in small volume blood samples. A key feature of many rapid tests is that they are dependent on the choice of sero-positivity cutoff, and there may be substantial misclassification for antibody levels close to this cutoff.

Antibody levels are not constant, and change over time. The early kinetics of the antibody response to SARS-CoV-2 have been well documented with a rapid rise in antibody levels occurring 5-15 days after symptom onset leading to sero-conversion (depending on the choice of cutoff) [1,6-9]. There are not yet data on the long-term kinetics of the SARS-CoV-

medRxiv preprint doi: https://doi.org/10.1101/2020.05.07.20093963.this version posted May 11, 2020. The copyright holder for this preprint (which was not certified by peer review) is the author/funder, who has granted medRxiv a license to display the preprint in perpetuity. It is made available under a CC-BY-NC-ND 4.0 International license .

2 antibody response. Assuming the antibody response is similar to that of other pathogens [10-14], we expect to observe a bi-phasic pattern of decay, with rapid decay in the first 3-6 months after infection, followed by a slower rate of decay. Notably, this decay pattern may lead to sero-reversion whereby a previously sero-positive individual reverts to being sero-negative. If a serological test with an inappropriately high choice of cutoff is used for SARS-CoV-2 serological surveys, there is a major risk that sero-reversion may lead to previously infected individuals testing sero-negative [15].

The antibody response generated following SARS-CoV-2 infection is diverse, consisting of multiple isotypes targeting several proteins on the virus surface including the spike protein (and its receptor binding domain) and the nucleoprotein [16]. This complexity of biomarkers provides both a challenge and an opportunity for diagnostics research. The challenge lies in selecting appropriate biomarkers and choosing between the increasing number of commercial assays, many of which have not been extensively validated and may produce conflicting results. The opportunity is that with multiple biomarkers, it is possible to generate a serological signature of infection that is robust to how antibody levels change over time [17-20], rather than relying on classification of sero-positive individuals using a single cutoff antibody level.

In this analysis, we apply mathematical models of antibody kinetics to serological data from the early stages of SARS-CoV-2 infection and predict the potential consequences for serological diagnostics within the first year following infection.

medRxiv preprint doi: https://doi.org/10.1101/2020.05.07.20093963.this version posted May 11, 2020. The copyright holder for this preprint (which was not certified by peer review) is the author/funder, who has granted medRxiv a license to display the preprint in perpetuity. It is made available under a CC-BY-NC-ND 4.0 International license .

# Methods

### Samples

We analysed 97 serum samples from 53 patients admitted to hospitals in Paris with SARS-CoV-2 infection confirmed by RT-qPCR [21,22], and 162 serum samples from healthcare workers in hospitals in Strasbourg (Table 1). 335 samples collected before December 2019 were used as negative controls. Samples from patients with RT-qPCR confirmed SARS-CoV-2 infection underwent a viral inactivation protocol by heating at 56 °C for 30 minutes. Negative control samples did not undergo the viral inactivation protocol. Serum samples positive for anti-malaria IgG antibodies were tested before and after the inactivation protocol. The viral inactivation protocol did affect measured IgG levels (data not shown). Notably, we did not assess the potential effect of the viral inactivation protocol on measured IgM levels.

**Table 1: Serum samples.** Positive control serum samples are from patients with RT-qPCR confirmed SARS-CoV-2 infection. Negative control samples are from panels collected pre-epidemic cohorts with ethical approval for broad antibody testing.

| Source | RT-qPCR confirmed | N: participants | N: samples |
|---|---|---|---|
| Hôpital Bichat, Paris | Yes | 4 | 34 |
| Nouvel Hôpital Civil & Hôpital de Haute Pierre, Strasbourg | Yes | 162 | 162 |
| Hôpital Cochin, Paris | Yes | 49 | 63 |
| Thai Red Cross | pre-epidemic negative controls | 68 | 68 |
| Peru negative controls | pre-epidemic negative controls | 90 | 90 |
| France blood donor (Établissement français du sang) | pre-epidemic negative controls | 177 | 177 |

### Serological assays

Four antigens derived from SARS-CoV-2 S protein were used. This includes $S^{tri}$ and RBD, produced as recombinant proteins in mammalian cells in the Structural Virology Unit at Institut Pasteur. S1 (cat# REC31806) and S2 (cat# REC31807) were purchased from Native Antigen, Oxford, UK. Protein were coupled to magnetic beads as described elsewhere [23]. The protein concentrations were optimized to generate a log-linear standard curve with a positive serum pool prepared from RT-qPCR-confirmed SARS-CoV-2 patients. The multiplex immunoassay was validated by comparing its performance when running in evaluated in singleplex format.

Recombinant SARS-CoV-2 trimeric Spike ectodomain ($S^{tri}$) and its RBD were designed based on the viral genome sequence of the SARS-CoV-2 strain France/IDF0372/2020, obtained from the GISAID database (accession number EPI_ISL_406596). The synthetic genes, codon-optimized for protein expression in mammalian cells, were ordered from GenScript and cloned in pcDNA3.1(+) vector as follows: the RBD, residues 331-519, and the entire S ectodomain (residues 1-1208). The RBD construct included an exogenous signal peptide of a human kappa light chain (METDTLLLWVLLLWVPGSTG) to ensure efficient protein secretion into the media. The S ectodomain construct was engineered, as reported before to have the stabilizing double proline mutation (KV986-987 to PP986-987) and the foldon domain at the C-terminus that allows the S to trimerize (YIPEAPRDGQAYVRKDGEWVLLSTFL) resembling the native S state on the virion [24]. Both constructs

medRxiv preprint doi: https://doi.org/10.1101/2020.05.07.20093963.this version posted May 11, 2020. The copyright holder for this preprint (which was not certified by peer review) is the author/funder, who has granted medRxiv a license to display the preprint in perpetuity. It is made available under a CC-BY-NC-ND 4.0 International license .

contained a Strep (WSHPQFEK), an octa-histidine, and an Avi tag (GLNDIFEAQKIEWHE) at the C-terminus for affinity purification. Protein expression was done by transient transfection of mammalian HEK293 free style cells, as already reported. Proteins were then purified from supernatants on a Streptactin column (IBA Biosciences) followed by size exclusion purification on Superdex 200 column using standard chromatography protocols.

In a black, 96 well, non-binding microtiter plate (cat#655090; Greiner Bio-One, Germany) 50 uL of protein-conjugated magnetic beads (500/region/uL) and 50 uL of diluted serum were mixed using a pipette and incubated for 30 min at room temperature on a plate shaker. All dilutions were made in phosphate buffered saline containing 1% bovine serum albumin and 0.05% (v/v) Tween-20 (denoted as PBT), and all samples were run in singlicate. Following incubation, the magnetic beads were separated using magnetic plate separator (Luminex®) for 60 seconds and washed thrice with 100 µl PBT using a multichannel pipette. The washed magnetic beads were incubated for 15 minutes with detector secondary antibody at room temperature on a plate shaker. The magnetic beads were separated and washed thrice with 100 µl PBT and finally resuspended in 100 µL of PBT.

For IgG measurements, samples were diluted at 1/100, and R-Phycoerythrin-(R-PE) conjugated Donkey Anti-Human IgM (Fc5µ ) F(ab')2 (cat#709-116-073; JacksonImmunoResearch, UK) antibody was used as detector antibody at 1/120 dilution. For IgM measurements, samples were diluted at 1/200, and R-Phycoerythrin -(R-PE) Donkey Anti-Human IgG (Fcγ) F(ab')2 (cat#709-116-098; JacksonImmunoResearch, UK) antibody was used as detector antibody at 1/400 dilution.

A positive control pool of serum at two-fold serial dilutions from 1:50 to 1:25,600 was included on each 96 well plate. Plates were read using a Luminex® MAGPIX® system which provides a reading of median fluorescence intensity (MFI). A 5-parameter logistic curve was used to convert measurements from MFI to antibody dilution.

**Statistical evaluation of diagnostic performance**

For measured antibody responses to a single antigen, diagnostic sensitivity is defined to be the proportion of patients with RT-qPCR confirmed SARS-CoV-2 infection with measured antibody levels above a given sero-positivity cutoff. Diagnostic specificity is defined to be the proportion of negative controls (with no history of SARS-CoV-2 infection) with measured antibody levels below a given sero-positivity cutoff. Sensitivity and specificity can be traded off against each other by varying the sero-positivity cutoff. This trade off is formally evaluated using Receiver Operating Characteristic (ROC) analysis. Measured antibody responses to multiple antigens can be combined to identify individuals with previous SARS-CoV-2 infection using classification algorithms. Here we use a random forests algorithm [17].

medRxiv preprint doi: https://doi.org/10.1101/2020.05.07.20093963.this version posted May 11, 2020. The copyright holder for this preprint (which was not certified by peer review) is the author/funder, who has granted medRxiv a license to display the preprint in perpetuity. It is made available under a CC-BY-NC-ND 4.0 International license .

**Mathematical model of antibody kinetics**

SARS-CoV-2 antibody kinetics are described using a previously published mathematical model of the immunological processes underlying the generation and waning of antibody responses following infection or infection [10]. The existing model is adapted to account for the frequent data available in the first weeks of infection.

$$\frac{dM}{dt} = -\delta M,$$
$$\frac{dB_s}{dt} = \rho M - c_s B_s,$$
$$\frac{dB_l}{dt} = (1-\rho)M - c_l B_l,$$
$$\frac{dA}{dt} = gB_s + gB_l - rA$$

where $M$ denotes memory B cells, δ is the rate of differentiation of memory B cells into antibody secreting plasma cells (ASC), $B_s$ denotes short-lived ASCs, $B_l$ denotes long-lived ASCs, $\rho$ is the proportion of ASCs that are short-lived, $g$ is the rate of generation of antibodies (IgG or IgM) from ASCs, and $r$ is the rate of decay of antibody molecules. Assuming $M(0) = M_0$ and $B_s(0) = B_l(0) = A(0) = 0$, these equations can be solved analytically to give:

$$A(t) = gM_0\left(\frac{(\rho c_l + (1-\rho)c_s - \delta)e^{-\delta t}}{(c_s-\delta)(c_l-\delta)(r-\delta)} + \frac{(\rho c_l + (1-\rho)c_s - r)e^{-rt}}{(c_s-r)(c_l-r)(\delta-r)} + \frac{\rho e^{-c_s t}}{(c_s-r)(c_s-\delta)} + \frac{(1-\rho)e^{-c_l t}}{(c_l-r)(c_l-\delta)}\right)$$

Statistical inference was implemented within a mixed-effects framework which allowed for characterisation of the kinetics within each individual while also describing the population-level patterns. On the population level, both the mean and variation in antibody kinetics are accounted for. The models were fitted in a Bayesian framework using Markov chain Monte Carlo methods with informative priors. Posterior parameter estimates are presented as medians with 95% credible intervals (CrIs).

**Prior data**

The recent emergence of SARS-CoV-2 means that long-term data on the duration of antibody responses do not yet exist. Therefore, predictions of antibody levels beyond the period for which data has been collected will be heavily dependent on structural model assumptions and assumed prior information. The prior estimate of the half-life of IgG molecules is 21 days. The prior estimate of the half-life of IgM molecules is 10 days. Prior estimates for the short-lived component of the antibody response (half-life = 3.5 days) are consistent with data from several sources [10-14]. The most notable uncertainty relates to estimates of the duration of the long-lived component of the SARS-CoV-2 antibody responses. We reviewed data from a number of sources on the long-term antibody kinetics following infection with other coronaviruses [25-30], summarized in Table S1. Based on the wide range of long-term antibody kinetics were observed, we assumed a prior estimate of the half-life of the long-lived component of the IgG antibody response to be 400 days, and that the proportion of the short-lived antibody secreting cells is 90%. This corresponds to a scenario where the IgG antibody

medRxiv preprint doi: https://doi.org/10.1101/2020.05.07.20093963.this version posted May 11, 2020. The copyright holder for this preprint (which was not certified by peer review) is the author/funder, who has granted medRxiv a license to display the preprint in perpetuity. It is made available under a CC-BY-NC-ND 4.0 International license .

responses decreases by approximately 60% after one year. Additional sensitivity analyses were run assuming the half-life of the long-lived component of the IgG antibody response to be 200 days and 800 days.

The model was first fitted to data from 23 patients with RT-qPCR confirmed SARS-CoV-2 infection in Hong Kong hospitals who were followed longitudinally for up to four weeks after initial onset of symptoms [1]. Posterior estimates from this model and data were used to provide prior estimates for the parameters describing the early stages of the antibody response (Table S2).

**Ethics**

Serum samples were obtained through the CORSER study (Etude séro-épidémiologique du virus SARS-CoV-2 en France : constitution d'une collection d'échantillons biologiques humains) directed by Institut Pasteur and approved by the Comité de Protection des Personnes Ile de France III, and the French COVID cohort (NCT04262921, sponsored by Inserm and approuved by the Comité de Protection des Personnes Ile de France VI). Use of the Peruvian negative controls was approved by the Institutional Ethics Committee from the Universidad Peruana Cayetano Heredia (UPCH) (SIDISI 100873).

medRxiv preprint doi: https://doi.org/10.1101/2020.05.07.20093963.this version posted May 11, 2020. The copyright holder for this preprint (which was not certified by peer review) is the author/funder, who has granted medRxiv a license to display the preprint in perpetuity. It is made available under a CC-BY-NC-ND 4.0 International license .

# Results

## Single biomarker classification

IgG and IgM antibody responses to $S^{tri}$, RBD, S1 and S2 were measured as median fluorescence intensity (MFI) and converted to antibody dilutions (Figure 1). For all eight biomarkers, measured responses were significantly higher in samples with RT-qPCR confirmed infection than in negative control samples (Figure 1A-H; P value < $1 \times 10^{-7}$; 2 sided t test).

The trade-off between sensitivity and specificity obtained by varying the cutoff for sero-positivity was investigated using a receiver operating characteristic (ROC) curve (Figure 1I). Depending on the characteristics of the desired diagnostic test, different targets for sensitivity and specificity can be considered. The results of three targets are summarized in Table 2. These are: (i) high sensitivity target where we enforce sensitivity > 99%; (ii) balanced sensitivity and specificity where both are approximately equal; and (iii) high specificity target where we enforce specificity >99%. Focusing on the high specificity target, using IgG to each of the four antigens we can obtain 99.1% specificity (95% CI: 97.4%, 99.7%) but with varying sensitivity: 90.3% (95% CI: 86.1%, 93.4%) for anti-Spike IgG; 76.4% (95% CI: 70.9%, 81.2%) for anti-RBD IgG; 49.4% (95% CI: 43.4%, 55.5%) for anti-S1 IgG; and 65.3% (95% CI: 59.3%, 70.8%) for anti-S2 IgG.

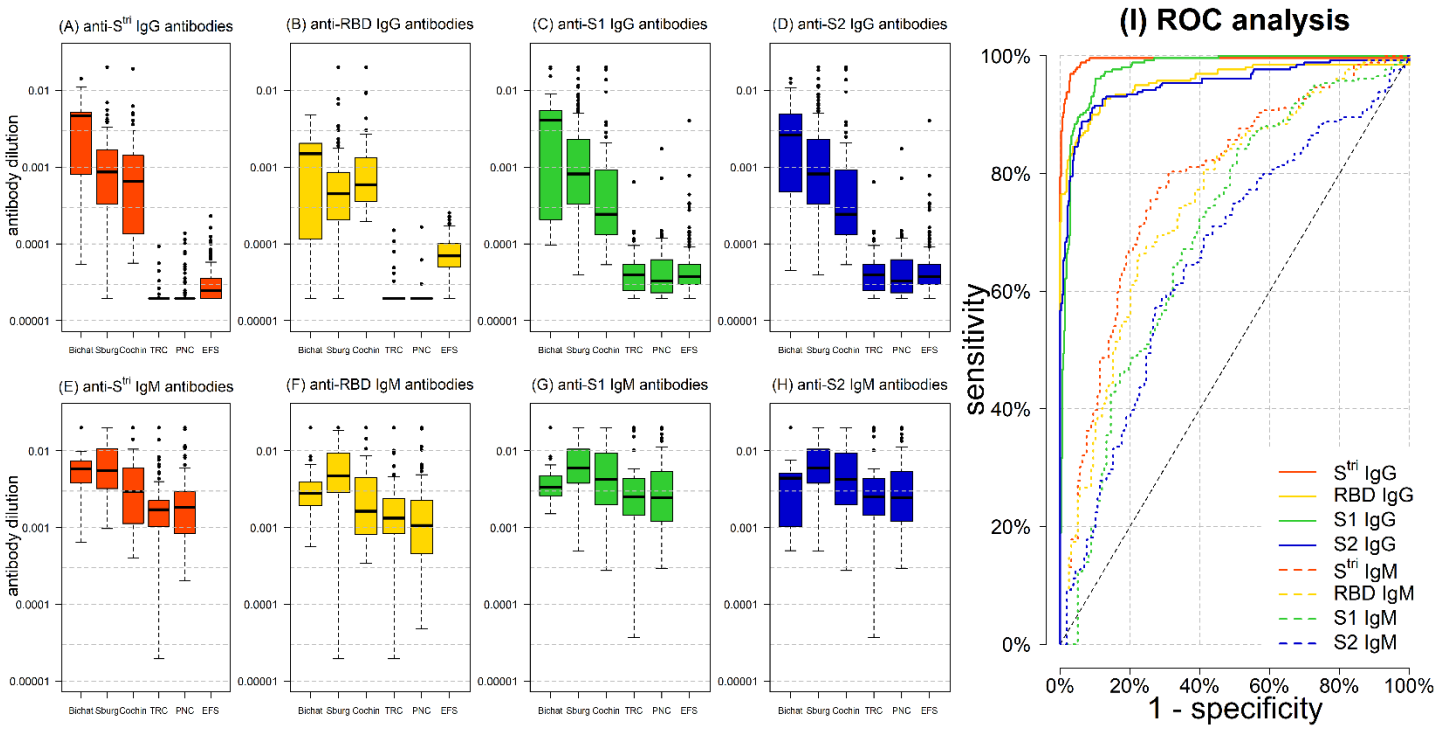


**Figure 1: Anti-SARS-CoV-2 antibody responses. (A-D)** Measured IgG antibody dilutions to $S^{tri}$, RBD, S1 and S2 in serum samples with previously confirmed RT-qPCR infection from patients in Hôpital Bichat (*n* = 34), health care workers in Nouvel Hôpital Civil & Hôpital de Haute Pierre, Strasbourg (*n* = 162), and Hôpital Cochin (*n* = 63). Negative control serum samples from Thailand (*n* = 68), Peru (*n* = 90), and French donors (*n* – 177) were also tested. **(E-H)** Measured IgM antibody dilutions to $S^{tri}$, RBD, S1 and S2 in serum samples. **(I)** Receiver Operating Characteristic (ROC) curve obtained by varying the cutoff for sero-positivity. IgG is shown with solid lines. IgM is shown with dashed lines.

medRxiv preprint doi: https://doi.org/10.1101/2020.05.07.20093963.this version posted May 11, 2020. The copyright holder for this preprint (which was not certified by peer review) is the author/funder, who has granted medRxiv a license to display the preprint in perpetuity. It is made available under a CC-BY-NC-ND 4.0 International license .

A high-specificity target was not possible using IgM antibodies to single antigens, with the exception of the trivial case of 100% specificity and 0% sensitivity. The poorer classification performance of IgM antibodies is a consequence of the smaller relative difference in measurements between positive and negative sample, compared to IgG antibodies. This may be due to the effects of heating during the viral inactivation protocol. Experiments are ongoing to assess this.

**Table 2: Sensitivity and specificity targets for single biomarkers.** 95% binomial confidence intervals were calculated using Wilson's method.

| biomarker | high sensitivity target (sensitivity > 99%) | | balanced target (sensitivity ~ specificity) | | high specificity target (specificity > 99%) | |
|---|---|---|---|---|---|---|
| | sensitivity | specificity | sensitivity | specificity | sensitivity | specificity |
| anti-$S^{tri}$ IgG | 99.2% (97.2%, 99.8%) | 92.5% (89.2%, 94.9%) | 96.9% (94.0%, 98.4%) | 97.0% (94.6%, 98.4%) | 90.3% (86.1%, 93.4%) | 99.1% (97.4%, 99.7%) |
| anti-RBD IgG | 100% (98.5%, 100%) | 0% (0%, 1.1%) | 90.0% (85.7%, 93.1%) | 89.9% (86.2%, 92.6%) | 76.4% (70.9%, 81.2%) | 99.1% (97.4%, 99.7%) |
| anti-S1 IgG | 99.2% (97.2%, 99.8%) | 75.8% (71.0%, 80.1%) | 91.5% (87.5%, 94.3%) | 91.6% (88.2%, 94.2%) | 49.4% (43.4%, 55.5%) | 99.1% (97.4%, 99.7%) |
| anti-S2 IgG | 99.2% (97.2%, 99.8%) | 22.7% (18.5%, 27.5%) | 90.7% (86.6%, 93.7%) | 90.7% (87.2%, 93.4%) | 65.3% (59.3%, 70.8%) | 99.1% (97.4%, 99.7%) |
| anti- $S^{tri}$ IgM | 100% (98.5%, 100%) | 7.0% (3.9%, 12.0%) | 73.7% (68.1%, 78.7%) | 74.1% (66.7%, 80.3%) | 0% (0%, 1.5%) | 100% (97.6%, 100%) |
| anti-RBD IgM | 99.2% (97.2%, 99.8%) | 12.7% (8.3%, 18.7%) | 69.9% (64.0%, 75.1%) | 69.6% (62.1%, 76.3%) | 0% (0%, 1.5%) | 100% (97.6%, 100%) |
| anti-S1 IgM | 99.6% (97.8%, 99.9%) | 1.3% (0.3%, 4.5%) | 65.3% (59.3%, 70.8%) | 65.2% (57.5%, 72.2%) | 0% (0%, 1.5%) | 100% (97.6%, 100%) |
| anti-S2 IgM | 99.2% (97.2%, 99.8%) | 0.6% (0.1%, 3.5%) | 63.7% (57.7%, 69.3%) | 63.9% (56.2%, 71.0%) | 0% (0%, 1.5%) | 100% (97.6%, 100%) |

**Serological signatures and multiple biomarker classification**

With eight biomarkers, there are 28 possible pairwise comparisons. Figure 2A-D provides an overview of four of these pairwise comparisons of antibody responses. The data are noisy, highly correlated and high dimensional (although only two dimensions are depicted here). We refer to the pattern of multiple antibody responses in multiple dimensions as the serological signature. Notably, there are two distinct clusters across all plots: antibody responses from negative control serum in blue cluster in the bottom left, and antibody responses from serum samples from individuals with RT-qPCR confirmed SARS-CoV-2 infection cluster in the centre and top right.

A random forests algorithm was used to formally classify these samples as positive or negative. The classification performance based on IgG antibody responses to the four antigens is shown with the ROC curves in Figure 2E. Using data from multiple biomarkers can lead to significant improvements in classification performance (Table 3). For example, for the high specificity target, with a single biomarker (anti-$S^{tri}$ IgG) we can achieve 99.1% specificity (95% CI: 97.4%, 99.1%) and 90.3% sensitivity (95% CI: 86.1%, 93.4%). However, by combining four biomarkers we can achieve 99.1% specificity (95% CI: 97.4%, 99.1%) and 96.1% sensitivity (95% CI: 93.0%, 97.9%).

medRxiv preprint doi: https://doi.org/10.1101/2020.05.07.20093963.this version posted May 11, 2020. The copyright holder for this preprint (which was not certified by peer review) is the author/funder, who has granted medRxiv a license to display the preprint in perpetuity. It is made available under a CC-BY-NC-ND 4.0 International license .

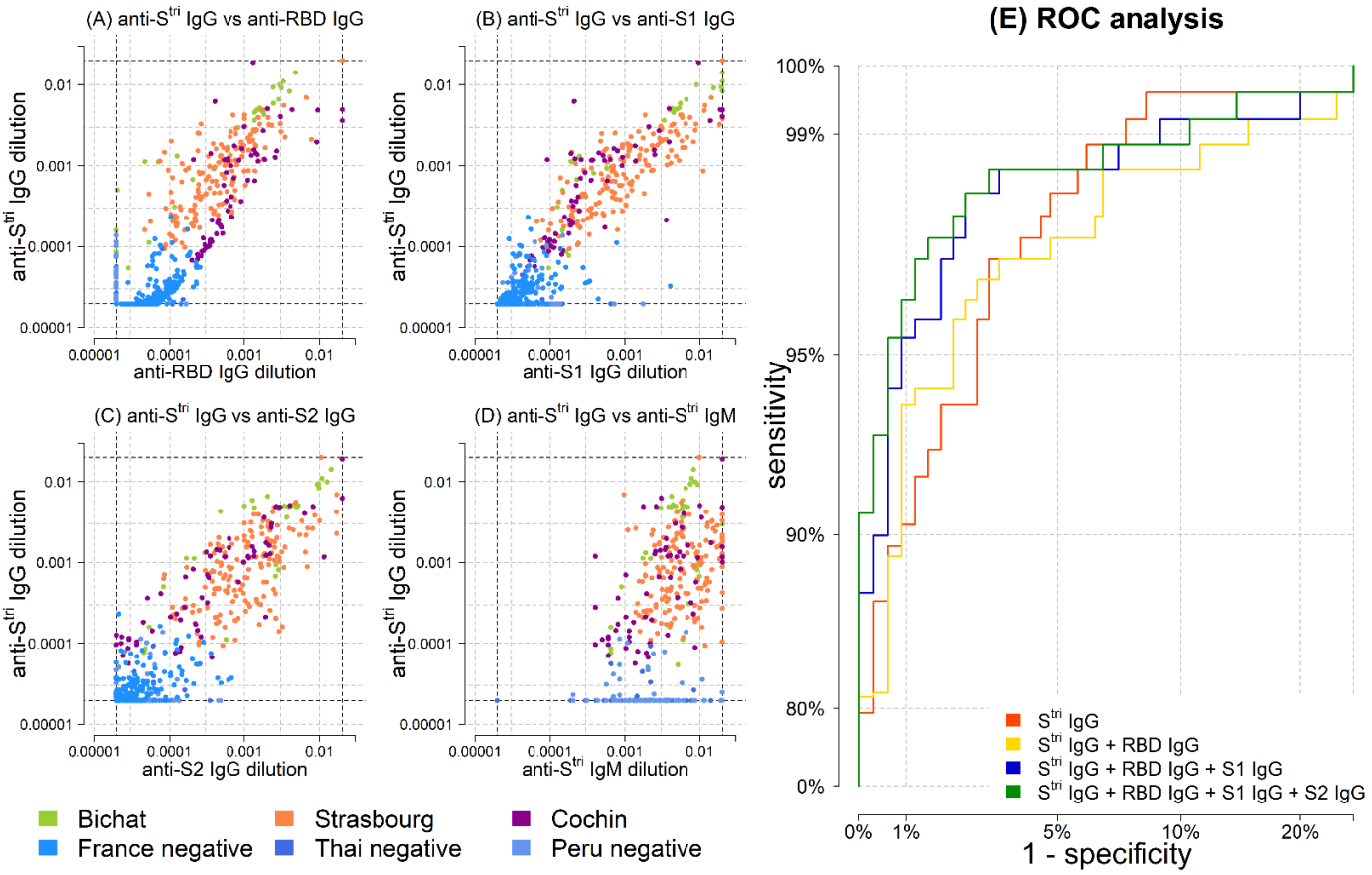


**Figure 2: Multiplex serological classification.** Anti-$S^{tri}$ IgG antibody dilution compared with **(A)** anti-RBD IgG antibody dilution; **(B)** anti-S1 IgG antibody dilution; **(C)** anti-S2 IgG antibody dilution; and **(D)** anti-$S^{tri}$ IgM antibody dilution. Each point denotes a measured antibody response from a sample from Hôpital Bichat (*n* = 34), Nouvel Hôpital Civil & Hôpital de Haute Pierre in Strasbourg (*n* = 162), and Hôpital Cochin (*n* = 63). Negative control serum samples are included from Thailand (*n* = 68), Peru (*n* = 90) and French blood donors (*n* =177). **(E)** ROC curve obtained by random forests multiple classification algorithm. Note that the axes have been rescaled to allow better visualization of the high sensitivity and high specificity region in the top left of the plot.

**Table 3: Sensitivity and specificity targets for multiple biomarkers.** Estimates of sensitivity and specificity are from a random forests classification algorithm. 95% binomial confidence intervals were calculated using Wilson's method.

| **antigen combination** | **high sensitivity target (sensitivity > 99%)** | | **balanced target (sensitivity ~ specificity)** | | **high specificity target (specificity > 99%)** | |
|---|---|---|---|---|---|---|
| | sensitivity | specificity | sensitivity | specificity | sensitivity | specificity |
| anti-$S^{tri}$ IgG | 99.2% (97.2%, 99.8%) | 92.5% (89.2%, 94.9%) | 96.9% (94.0%, 98.4%) | 97.0% (94.6%, 98.4%) | 90.3% (86.1%, 93.4%) | 99.1% (97.4%, 99.7%) |
| anti- $S^{tri}$ IgG + anti-RBD IgG | 99.2% (97.2%, 99.8%) | 85.7% (81.5%, 89.0%) | 96.5% (93.5%, 98.2%) | 96.7% (94.2%, 98.2%) | 93.8% (90.2%, 96.2%) | 99.1% (97.4%, 99.7%) |
| anti- $S^{tri}$ IgG + anti-RBD IgG + anti-S1 IgG | 99.2% (97.2%, 99.8%) | 91.0% (87.5%, 93.7%) | 97.7% (95.0%, 98.9%) | 97.6% (95.4%, 98.8%) | 95.4% (92.1%, 97.3%) | 99.1% (97.4%, 99.7%) |
| anti- $S^{tri}$ IgG + anti-RBD IgG + anti-S1 IgG + anti-S2 IgG | 99.2% (97.2%, 99.8%) | 89.6% (85.8%, 92.4%) | 97.7% (95.0%, 98.9%) | 97.6% (95.4%, 98.8%) | 96.1% (93.0%, 97.9%) | 99.1% (97.4%, 99.7%) |

medRxiv preprint doi: https://doi.org/10.1101/2020.05.07.20093963.this version posted May 11, 2020. The copyright holder for this preprint (which was not certified by peer review) is the author/funder, who has granted medRxiv a license to display the preprint in perpetuity. It is made available under a CC-BY-NC-ND 4.0 International license .

## SARS-CoV-2 antibody kinetics

A mathematical model of antibody kinetics was fit to the serological data. Figure 3 shows the data from patients from Hôpital Bichat with frequent longitudinal sampling. The predicted antibody kinetics are informed by prior data from 22 patients in Hong Kong hospitals [1]. The data and model indicate that the antibody response is in a rising phase between 5 and 15 days after symptom onset.

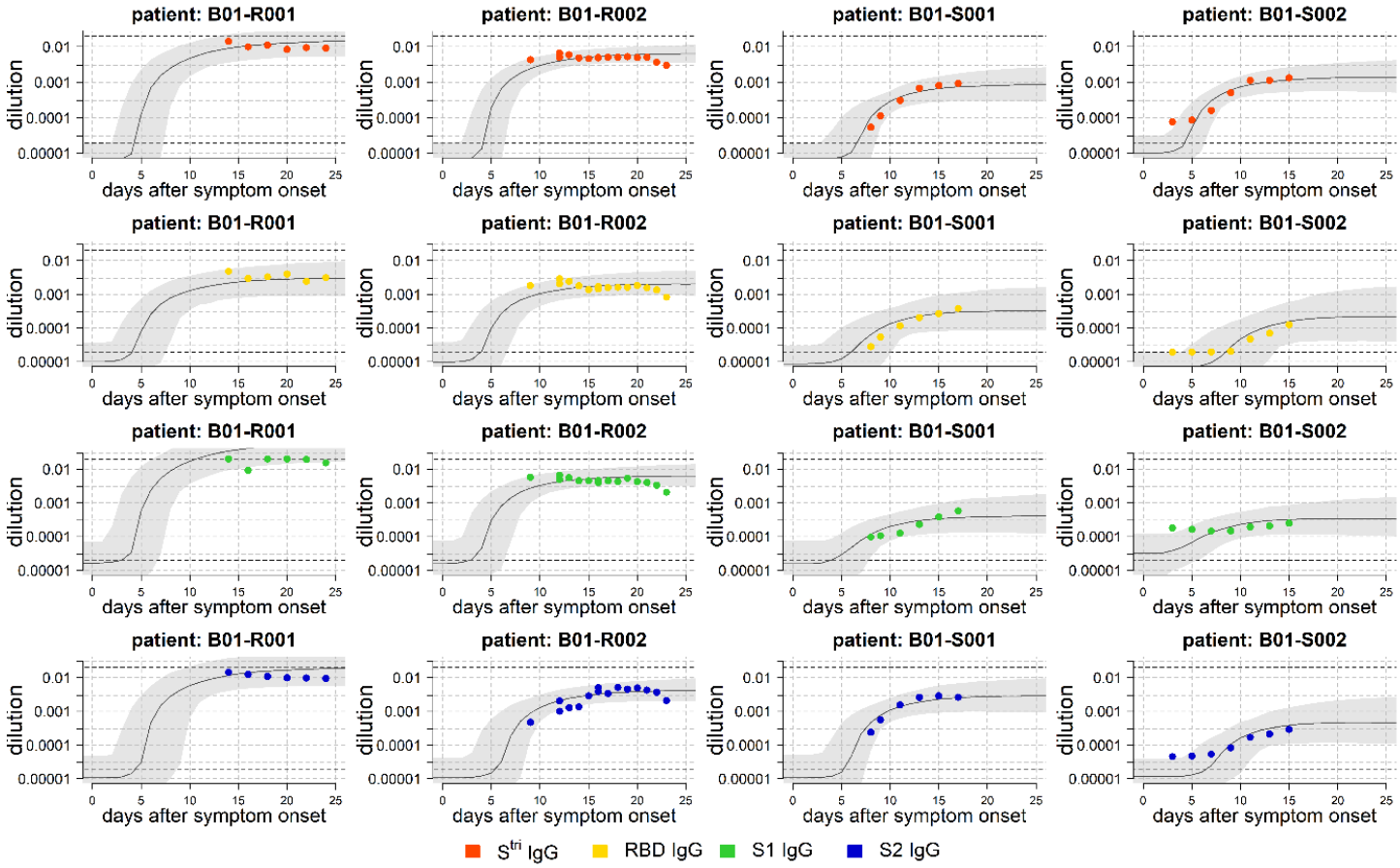


**Figure 3: Model fit to longitudinal data on IgG antibody kinetics.** Measured IgG antibody responses, shown as points, from four patients in Hôpital Bichat followed longitudinally for up to 24 days after symptom onset. Posterior median model predictions are shown as black lines, with 95% credible intervals in grey. The black horizontal dashed lines represent the upper and lower limits of the assay.

## Sensitivity of serological assays over time

Mathematical models of antibody kinetics were fitted to data on anti-SARS-CoV-2 antibody responses during the first month following symptom onset and informed by prior information on the long-term kinetics of antibody responses to other human coronaviruses. We predicted the anti-SARS-CoV-2 antibody response during the first year following symptom onset, with quantification of uncertainty. For each individual with RT-qPCR SARS-CoV-2 infection, Figure 4A-D shows the model predicted IgG antibody response to four antigens. For all four antigens, we predict a bi-phasic pattern of waning

medRxiv preprint doi: https://doi.org/10.1101/2020.05.07.20093963.this version posted May 11, 2020. The copyright holder for this preprint (which was not certified by peer review) is the author/funder, who has granted medRxiv a license to display the preprint in perpetuity. It is made available under a CC-BY-NC-ND 4.0 International license .

with a first rapid phase between one and three months after symptom onset, followed by a slower rate of waning. The percentage reduction in antibody level after one year was mostly determined by prior information and estimated to be 55% (95% CrI: 35%, 74%) for anti-$S^{tri}$ IgG antibodies, 56% (95% CrI: 33%, 78%) for anti-RBD IgG antibodies, 58% (95% CrI: 38%, 73%) for anti-S1 IgG antibodies, and 56% (95% CrI: 35%, 77%) for anti-$S^{tri}$ IgG antibodies.

Sensitivity was assessed using the sero-positivity cutoff based on the high specificity target in Table 2. For all antigens considered, we predict that there will be a reduction in sensitivity over time, although there is a large degree of uncertainty. In particular, we predict that the sensitivity based on anti-$S^{tri}$ IgG antibody responses after six months will be 97% (95% CrI: 79%, 100%); that sensitivity based on anti-RBD IgG antibody responses after six months will be 81% (95% CrI: 56%, 99%); that sensitivity based on anti-S1 IgG antibody responses after six months will be 56% (95% CrI: 40%, 80%); and that sensitivity based on anti-S2 IgG antibody responses after six months will be 80% (95% CrI: 60%, 95%).

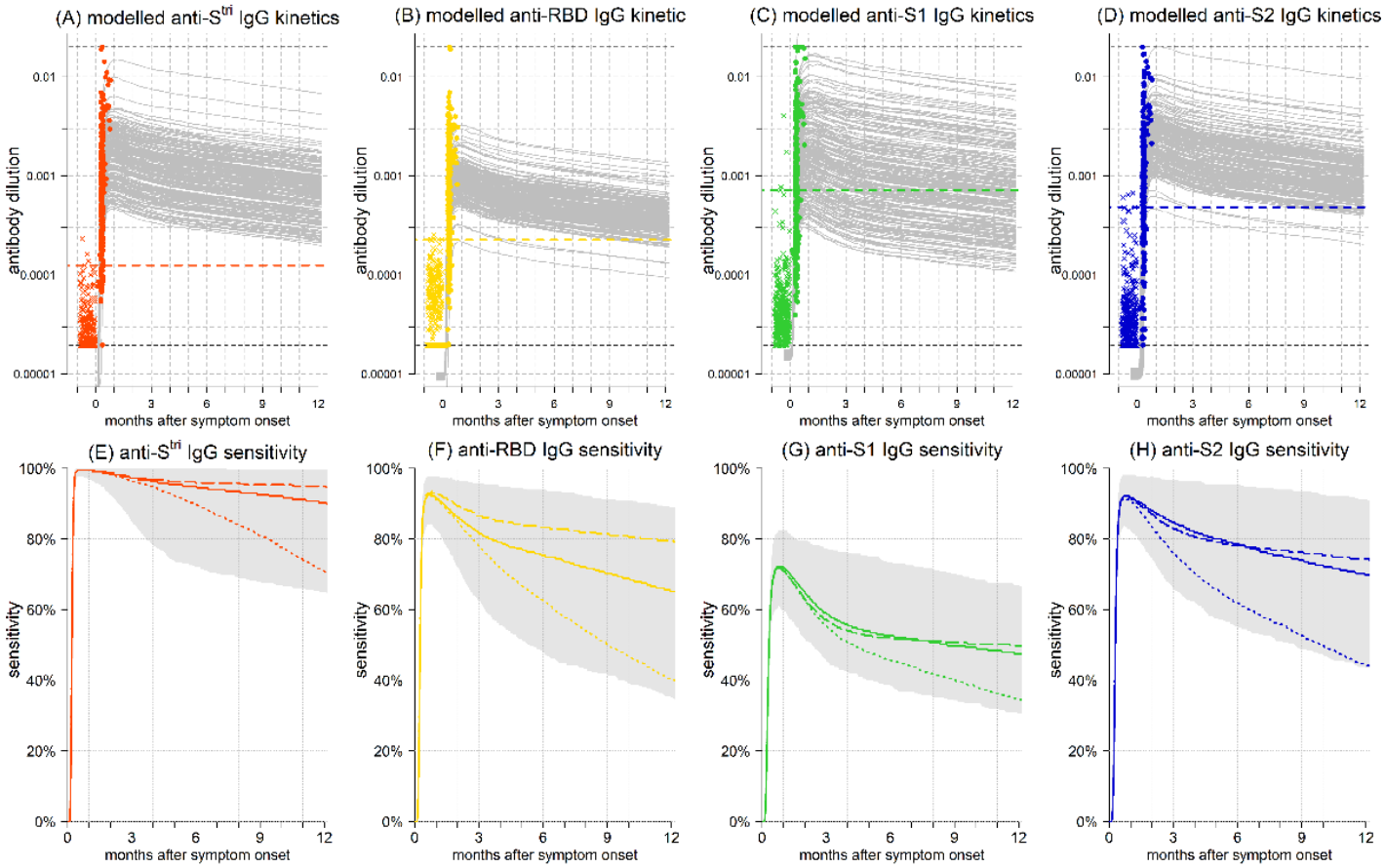


**Figure 4: Anti-SARS-CoV-2 antibody kinetics and sensitivity. (A-D)** Measured antibody levels in individuals with confirmed SARS-CoV-2 infection are depicted as points. Measured antibody levels in negative controls are depicted as crosses. Grey lines show posterior median model predictions from the scenario with prior information on long-term kinetics from other coronaviruses. The horizontal dashed line represents the high specificity target (99%) sero-positivity cutoff. **(E-F)** Estimated sensitivity over time for the high specificity target sero-positivity cutoff. The solid line represents the posterior model prediction. The dashed and dotted lines represent the posterior model predictions for the sensitivity analyses assuming prior information for a longer or shorter duration of the long-lived component of the antibody responses. Grey shaded regions denote the 95% credible intervals.

medRxiv preprint doi: https://doi.org/10.1101/2020.05.07.20093963.this version posted May 11, 2020. The copyright holder for this preprint (which was not certified by peer review) is the author/funder, who has granted medRxiv a license to display the preprint in perpetuity. It is made available under a CC-BY-NC-ND 4.0 International license .

### Modelling the long-term serological signature

The evolution of the serological signature over time can be predicted using mathematical models of antibody kinetics (Figure 5). Notably, in the absence of long-term longitudinal data there is too much uncertainty to make confident predictions. Nonetheless, modelling allows us to anticipate a number of likely qualitative behaviours. For samples taken in the first few weeks after symptom onset, the serological signature will be noisy as many individuals may still be in the phase where antibody levels are still rising (Figure 5A). Once the rising phase of antibody responses has completed in all individuals, we predict a clear serological signature as shown in Figure 5B. Once antibody levels have peaked, we predict that waning antibody levels over time will cause the cluster of positive responses to move closer to the cluster of negative antibody responses (Figure 5C,D). Notably, there is substantial uncertainty, both in terms of each individual's antibody response, and in terms of the behaviour of antibody kinetics across the entire population.

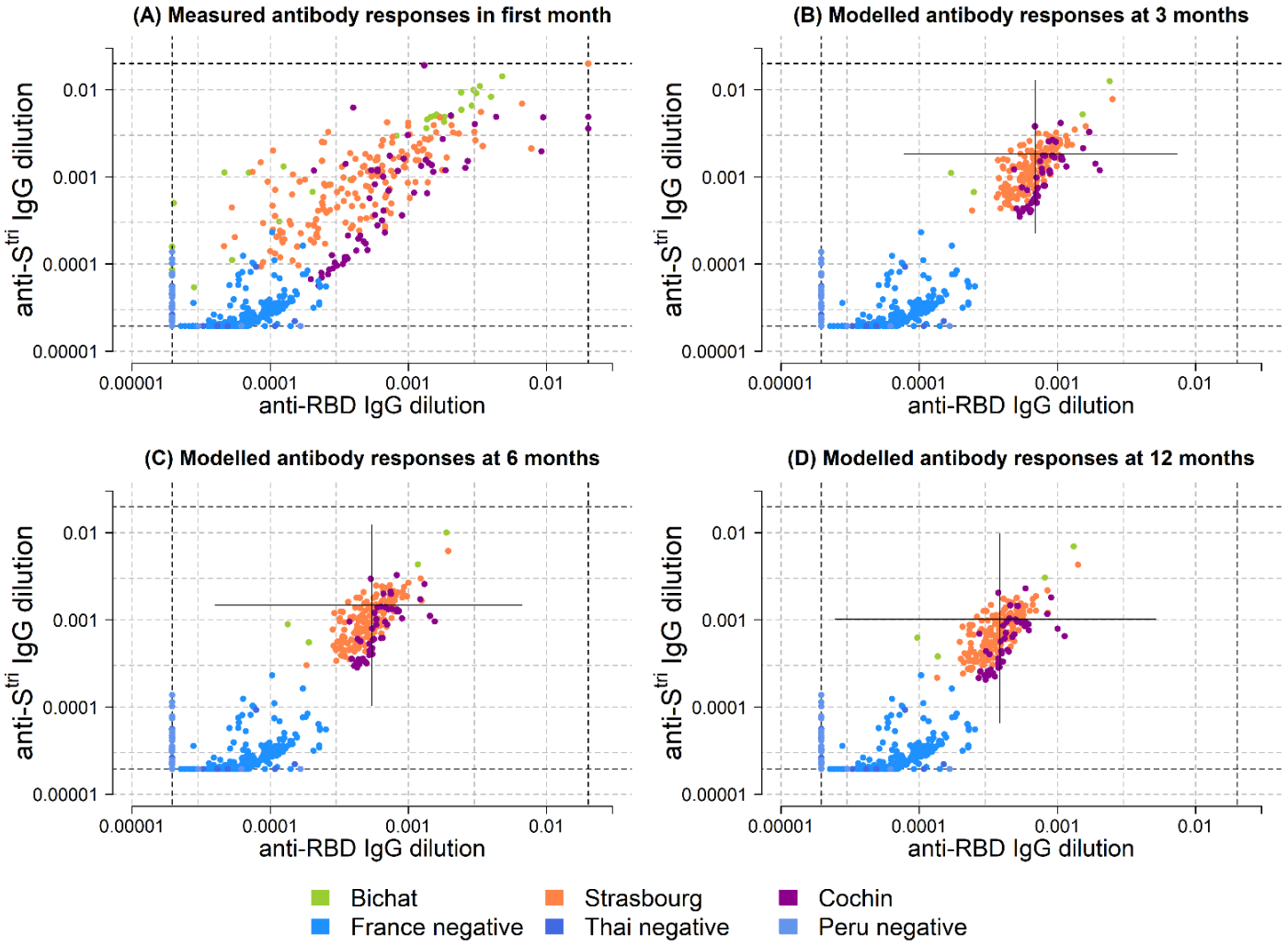


**Figure 5: Evolution of serological signature over time. (A)** Measured anti-$S^{tri}$ and anti-RBD IgG antibody responses. Model predicted anti- $S^{tri}$ and anti-RBD IgG antibody responses at: **(B)** 3 months after symptom onset; **(C)** 6 months after symptom onset; and **(D)** 12 months after symptom onset. Predictions were made using a mathematical model of antibody kinetics with prior information on long-term kinetics based on SARS-CoV. For one randomly selected data point, the model uncertainty is depicted via the black cross.

medRxiv preprint doi: https://doi.org/10.1101/2020.05.07.20093963.this version posted May 11, 2020. The copyright holder for this preprint (which was not certified by peer review) is the author/funder, who has granted medRxiv a license to display the preprint in perpetuity. It is made available under a CC-BY-NC-ND 4.0 International license .

# Discussion

Infection with SARS-CoV-2 induces antibodies of multiple isotypes (IgG, IgM, IgA) targeting multiple epitopes on spike proteins exposed on the virus surface, and nucleoprotein. Each of these biomarkers may exhibit distinct kinetics leading to variation in their potential diagnostic performance. There is also substantial between-individual variation in the antibody response generated following SARS-CoV-2 infection. By measuring multiple biomarkers in large numbers of individuals, it is possible to create a serological signature of previous infection [17-19]. Although necessarily more complex than a single measured antibody response, such an approach has the potential of providing more accurate classification and being more stable over time.

The long-term kinetics of the antibody response to SARS-CoV-2 won't be definitively quantified until infected individuals are followed longitudinally for months and even years after RT-qPCR confirmed infection. As of May 2020, the longest possible follow-up time after symptoms is four to five months. As we wait for this data to be collected, mathematical models can provide important insights into how SARS-CoV-2 antibody levels may change over time. Modelling beyond the timeframe for which we have data has its limitations, however our approach benefits from robust quantification of uncertainty accounting for a wide range of future scenarios. Furthermore, this modelling approach provides falsifiable predictions which will allow models to be updated as our team and others generate new data. For the purpose of evaluation of antibody kinetics, measured antibody responses from samples collected from individuals followed longitudinally after confirmed SARS-CoV-2 infection will be especially valuable.

The simulations presented here predict that following SARS-CoV-2 infection, antibody responses will increase rapidly 1-2 weeks after symptom onset, with antibody responses peaking within 2-4 weeks. After this peak, antibody responses are predicted to decline according to a bi-phasic pattern, with rapid decay in the first three to six months followed by a slower rate of decay. Model predictions of the rise and peak of antibody response are informed by, and are consistent with, many sources of data [10-14,31]. Model predictions of the decay of antibody responses are strongly determined by prior information on longitudinal follow-up of individuals infected with other coronaviruses [25-30]. Under the scenario that the decay of SARS-CoV-2 antibody responses is similar to that of SARS-CoV, we would expect substantial reductions in antibody levels within the first year after infection. For the sero-positivity cutoffs highlighted here, this could cause approximately 50% of individuals to test sero-negative after one year, depending on the exact choice of biomarker and sero-positivity cut-off.

This presents a potential problem for SARS-CoV-2 serological diagnostics. Most commercially available diagnostic tests compare antibody responses to a fixed sero-positivity cutoff. Where these cutoffs have been validated, it is typically by comparison of serum from negative control samples collected pre-epidemic with serum from hospitalized patients in the first weeks of infection (i.e. when antibody responses are likely to be at their highest) [32,33]. If we fail to account for antibody kinetics, we risk incorrectly classifying individuals with old infections (e.g. >6 months) as sero-negative. This is particularly important for commercially available point-of-care rapid serological tests with fixed cutoffs, limited dynamic

medRxiv preprint doi: https://doi.org/10.1101/2020.05.07.20093963.this version posted May 11, 2020. The copyright holder for this preprint (which was not certified by peer review) is the author/funder, who has granted medRxiv a license to display the preprint in perpetuity. It is made available under a CC-BY-NC-ND 4.0 International license .

range and visual evaluation. If inappropriate tests are used in sero-prevalence surveys, there is a risk of substantial under-estimation of the proportion of infected individuals.

It is often impossible to have both high sensitivity and high specificity, and we must select an appropriate trade-off. For sero-surveillance of pathogens with low prevalence (<20%), we recommend prioritizing specificity. For example, if the true sero-prevalence of SARS-CoV-2 in a population is 8%; a test with 100% sensitivity and 90% specificity would return an estimate of 1x8% + 0.1x92% = 17.2%, a substantial over-estimate. Due to the potential problem of false positives, we recommend aiming for a high specificity target of >99%. However, accurate validation of high sensitivity and high specificity serological diagnostic tests requires large number of samples. Many tests are validated on fewer than 100 samples [5], and this is not sufficient. Indeed, the 594 samples used in this analysis is also arguably not sufficient. Ideally, we would aim to validate on ~1,000 positive and ~1,000 negative samples. Furthermore, it is important to avoid testing on homogenous panels of samples. Obtaining samples from multiple panels with different epidemiological backgrounds will contribute to more robust validation.

There are a large number of immunological assays capable of measuring the antibody response to SARS-CoV-2 including neutrilization assays, ELISA, Luminex, Luciferase Immunoprecipitation System (LIPS), peptide microarrays and more [34]. From the perspective of quantifying protective immunity and vaccine development, functional approaches such as neutrilization assays are clearly preferable. However, from a surveillance and diagnostics perspective, assays should be assessed in terms of their performance at classifying individuals with a previous RT-qPCR confirmed infection. Put simply, if your wish is to diagnose someone, you don't care what a biomarker does, only that it can be reliably detected in previously infected individuals and not in uninfected individuals.

Beyond diagnostics, assessment of antibody kinetics may contribute to better understanding of the immune responses generated by SARS-CoV-2 vaccines. Statistical models can be used to identify immunological correlates of protection, at least according to conditions such as the Prentice criterion [35,36]. An estimated correlate of protection may take the form of a dose-response relationship, with higher antibody levels associated with greater vaccine efficacy. Under the assumption that a correlate of protection can be identified, models of antibody kinetics can be used to provide preliminary estimates of the duration of protection following vaccination or natural infection [13,37].

The analysis presented here is based on limited data, and the predictions may subsequently be contradicted as more data become available. However, the concepts outlined here of serological signatures of SARS-CoV-2 infection generated by multiplex assays, and mathematical models of antibody kinetics, allow us to plan in advance for some of the future challenges that we may face in SARS-CoV-2 serological surveillance.

medRxiv preprint doi: https://doi.org/10.1101/2020.05.07.20093963.this version posted May 11, 2020. The copyright holder for this preprint (which was not certified by peer review) is the author/funder, who has granted medRxiv a license to display the preprint in perpetuity. It is made available under a CC-BY-NC-ND 4.0 International license .

## Author contributions

JRS optimized protocols and processed samples. CC and CD processed samples. SM implemented inactivation protocols. MB and AM designed and produced antigens. SK, BT, SFK, and JdS collected samples. IM and MW developed the concept. MW analysed the data and wrote the manuscript.

## Acknowledgements

The French COVID cohort is supported by the REACTing consortium and by the French Directorate General for Health. Rhea Longley is thanked for her contribution to protocol development. Darragh Duffy, Jérôme Hadjadj and Laura Barnabei are thanked for their work on the Hôpital Cochin study. Arnaud Fontanet is thanked for critical reading of the manuscript. Dionicia Gamboa is thanked for sharing negative control samples from Peru. Jetsumon Sattabongkot is thanked for sharing negative control samples from Thailand. Marie-Noelle Ungeheuer and Blanca Liliana Perlaza are thanked for processing samples at the ICAReB platform in Institut Pasteur. Shane Mansfield and Richard Davison are thanked for their help in the solution of differential equations. We thank all patients and health care workers who kindly agreed for samples to be used for medical research purposes.

## Funding

This work was supported by the European Research Council (MultiSeroSurv ERC Starting Grant; MW), l'Agence Nationale de la Recherche and Fondation pour la Recherche Médicale (CorPopImm; MW), and the Institut Pasteur International Network (CoronaSeroSurv; MW).

## Code and Data Availability

All data and code used for reproducing the results is freely available on GitHub: https://github.com/MWhite-InstitutPasteur/SARSCoV2_sero_dx.

medRxiv preprint doi: https://doi.org/10.1101/2020.05.07.20093963.this version posted May 11, 2020. The copyright holder for this preprint (which was not certified by peer review) is the author/funder, who has granted medRxiv a license to display the preprint in perpetuity. It is made available under a CC-BY-NC-ND 4.0 International license .

# References


1. To KK, Tsang OT, Leung WS, Tam AR, Wu TC, Lung DC, *et al*. Temporal profiles of viral load in posterior oropharyngeal saliva samples and serum antibody responses during infection by SARS-CoV-2: an observational cohort study. *Lancet Infect Dis*. 2020; S1473-3099(20)30196-1.
2. Wölfel R, Corman VM, Guggemos W, Seilmaier M, Zange S, Müller MA, *et al*. Virological assessment of hospitalized patients with COVID-2019. *Nature*. 2020; doi: 10.1038/s41586-020-2196-x.
3. Siordia JA Jr. Epidemiology and clinical features of COVID-19: A review of current literature. *J Clin Virol*. 2020; 127:104357.
4. Migchelsen SJ, Martin DL, Southisombath K, Turyaguma P, Heggen A, Rubangakene PP, *et al*. Defining Seropositivity Thresholds for Use in Trachoma Elimination Studies. *PLoS Negl Trop Dis.* 2017; 11(1):e0005230.
5. SARS-CoV-2 diagnostics: performance data. The Foundation for Innovative New Diagnostics (FIND). https://www.finddx.org/covid-19/dx-data/
6. Guo L, Ren L, Yang S, *et al*. Profiling Early Humoral Response to Diagnose Novel Coronavirus Disease (COVID-19). *Clin Inf Dis*. 2020; https://doi.org/10.1093/cid/ciaa310
7. Okba NMA, Muller MA, Li W, *et al.* SARS-CoV-2 specific antibody responses in COVID-19 patients. *medRxiv*. 2020; doi: https://doi.org/10.1101/2020.03.18.20038059
8. Amanat F, Stadlbauer D, Strohmeier S, Nguyen T, Chromikova V, McMahon M, *et al*. A serological assay to detect SARS-CoV-2 seroconversion in humans. *medRxiv*. 2020; doi: https://doi.org/10.1101/2020.03.17.20037713
9. Huang AT, Garcia-Carreras B, Hitchings MDT, Yang B, Katzelnick L, Rattigan SM, *et al*. A systematic review of antibody mediated immunity to coronaviruses: antibody kinetics, correlates of protection, and association of antibody responses with severity of disease. *medRxiv*. 2020; doi: https://doi.org/10.1101/2020.04.14.20065771
10. White MT, Griffin JT, Akpogheneta O, *et al.* Dynamics of the antibody response to *Plasmodium falciparum* infection in African children. *J Infect Dis* 2014; 210: 1115–22.
11. Teunis PF, van Eijkeren JC, de Graaf WF, Marinović AB, Kretzschmar ME. Linking the seroresponse to infection to within-host heterogeneity in antibody production. *Epidemics* 2016; 16: 33–39.
12. Andraud M, Lejeune O, Musoro *et al*. Living on three time scales: the dynamics of plasma cell and antibody populations illustrated for hepatitis A virus. *PLoS Comput Biol* 2012; 8: e1002418.
13. White MT, Verity R, Griffin JT, *et al*. Immunogenicity of the RTS,S/AS01 malaria vaccine and implications for duration of vaccine efficacy: secondary analysis of data from a phase 3 randomised controlled trial. *Lancet Infect Dis* 2015; 15: 1450–58.
14. White MT, Bejon P, Olotu A, *et al.* A combined analysis of immunogenicity, antibody kinetics and vaccine efficacy from phase 2 trials of the RTS,S malaria vaccine. *BMC Med* 2014; 12: 117
15. Adams ER, Anand R, Andersson MI, Auckland K, Baillie JK, Barnes E, *et al*. Evaluation of antibody testing for SARS-Cov-2 using ELISA and lateral flow immunoassays. *medRxiv*. 2020; doi: https://doi.org/10.1101/2020.04.15.20066407
16. Hachim A, Kavian N, Cohen CA, Chin AWH, Chu DKW, Ka Pun Mok C, *et al*. Beyond the Spike: identification of viral targets of the antibody response to SARS-CoV-2 in COVID-19 patients. *medRxiv*. 2020; doi: https://doi.org/10.1101/2020.04.30.20085670
17. Longley RJ, White MT, Takashima E, Brewster J, Morita M, Harbers M, *et al*. Development and validation of serological markers for detecting recent exposure to *Plasmodium vivax* infection. *Nature Med*. 2020; (in press)
18. Azman AS, Lessler J, Luquero FJ, Bhuiyan TR, *et al*. Estimating cholera incidence with cross-sectional serology. *Sci Transl Med*. 2019; 11(480)

medRxiv preprint doi: https://doi.org/10.1101/2020.05.07.20093963.this version posted May 11, 2020. The copyright holder for this preprint (which was not certified by peer review) is the author/funder, who has granted medRxiv a license to display the preprint in perpetuity. It is made available under a CC-BY-NC-ND 4.0 International license .


19. Helb DA, Tetteh KK, Felgner PL, Skinner J, Hubbard A, Arinaitwe E, *et al*. Novel serologic biomarkers provide accurate estimates of recent Plasmodium falciparum exposure for individuals and communities. *Proc Natl Acad Sci USA*. 2015; 112(32):E4438-47
20. Perraut R, Varela ML, Loucoubar C, Niass O, Sidibé A, Tall A, *et al*. Serological signatures of declining exposure following intensification of integrated malaria control in two rural Senegalese communities. *PLoS One*. 2017; 12(6):e0179146
21. Hadjadj J, Yatim N, Barnabei L, Corneau A, Boussier J, Pere H, *et al*. Impaired type I interferon activity and exacerbated inflammatory responses in severe Covid-19 patients. *medRxiv*. 2020; doi: https://doi.org/10.1101/2020.04.19.20068015
22. Lescure FX, Bouadma L, Nguyen D, Parisey M, Wicky PH, Behillil S, *et al.* Clinical and virological data of the first cases of COVID-19 in Europe: a case series. *Lancet Inf Dis*. 2020; S1473-3099(20)30200-0
23. Longley RJ, França CT, White MT, Kumpitak C, Sa-Angchai P, Gruszczyk J, *et al.* Asymptomatic *Plasmodium vivax* infections induce robust IgG responses to multiple blood-stage proteins in a low-transmission region of western Thailand. *Malar J*. 2017; 16(1):178.
24. Kirchdoerfer RN, Wang N, Pallesen J, Wrapp D, Turner HL, Cottrell CA, *et al*. Stabilized coronavirus spikes are resistant to conformational changes induced by receptor recognition or proteolysis. *Sci Rep*. 2018; 8(1):15701
25. Callow KA, Parry HF, Sergeant M, Tyrrell DA. The time course of the immune response to experimental coronavirus infection of man. *Epidemiol Infect*. 1990; 105(2):435-46.
26. Wu LP, Wang NC, Chang YH, Tian XY, Na DY, Zhang LY, Zheng L, Lan T, Wang LF, Liang GD. Duration of antibody responses after severe acute respiratory syndrome. *Emerg Infect Dis.* 2007; 13(10): 1562-4.
27. Choe PG, Perera RAPM, Park WB, Song KH, Bang JH, Kim ES, *et al*. MERS-CoV antibody responses 1 year after symptom onset, South Korea, 2015. *Emerg Infect Dis.* 2017; 23(7):1079-1084.
28. Liu W, Fontanet A, Zhang PH, Zhan L, Xin ZT, Baril L, *et al*. Two-year prospective study of the humoral immune response of patients with severe acute respiratory syndrome. *J Infect Dis*. 2006; 193:792–5
29. Mo H, Zeng G, Ren X, Li H, Ke C, Tan Y, *et al.* Longitudinal profile of antibodies against SARS-coronavirus in SARS patients and their clinical significance. *Respirology*. 2006; 11(1):49-53.
30. Cao WC, Liu W, Zhang PH, Zhang F, Richardus JH. Disappearance of antibodies to SARS-associated coronavirus after recovery. *N Engl J Med*. 2007; 357(11):1162-3.
31. Yman V, White MT, Asghar M, Sundling C, Sondén K, Draper SJ, *et al*. Antibody responses to merozoite antigens after natural *Plasmodium falciparum* infection: kinetics and longevity in absence of re-exposure. *BMC Med*. 2019; 17(1):22
32. Long Q, Deng H, Chen J, *et al*. Antibody responses to SARS-CoV-2 in COVID-19 patients: the perspective application of serological tests in clinical practice. *MedRxiv*. 2020; https://doi.org/10.1101/2020.03.18.20038018
33. Lassaunière R, Frische A, Harboe ZB, Nielsen ACY, Fomsgaard A, Krogfelt KA, Jørgensen CS. Evaluation of nine commercial SARS-CoV-2 immunoassays. *medRxiv*. 2020; https://doi.org/10.1101/2020.04.09.20056325
34. Grzelak L, Temmam S, Planchais C, Demeret C, Huon C, Guivel F, *et al*. SARS-CoV-2 serological analysis of COVID-19 hospitalized patients, pauci-symptomatic individuals and blood donors. *medRxiv*. 2020; doi: https://doi.org/10.1101/2020.04.21.20068858
35. Prentice RL. Surrogate endpoints in clinical-trials—definition and operational criteria. *Stat Med* 1989; 8: 431–40.
36. Qin L, Gilbert PB, Corey L, McElrath MJ, Self SG. A framework for assessing immunological correlates of protection in vaccine trials. *J Infect Dis* 2007; 196: 1304–12.
37. White MT, Idoko O, Sow S, Diallo A, Kampmann B, Borrow R, Trotter C. Antibody kinetics following vaccination with MenAfriVac and implications for the duration of protection: an analysis of serological data. *Lancet Inf Dis*. 2019; 19(3):327-336

medRxiv preprint doi: https://doi.org/10.1101/2020.05.07.20093963.this version posted May 11, 2020. The copyright holder for this preprint (which was not certified by peer review) is the author/funder, who has granted medRxiv a license to display the preprint in perpetuity. It is made available under a CC-BY-NC-ND 4.0 International license .

# Supplementary Appendix: Mathematical modelling of the duration of the anti-SARS-CoV-2 antibody response

## Overview

There are limited available longitudinal data on SARS-CoV-2 antibody kinetics, and no data from long-term follow-up (as of May 2020). However, there are a number of published studies on the long-term antibody kinetics to other coronaviruses, most notably Severe Acute Respiratory Syndrome coronavirus (SARS-CoV). Here we review some of the available published data, and describe how this can be used to provide prior information for modelling SARS-CoV-2 antibody kinetics.

## Prior longitudinal data on long-term antibody responses to coronaviruses

Table S1 summarises some of the published data on the long-term antibody kinetics to a number of coronaviruses: SARS-CoV, human seasonal coronavirus 229E, and Middle East Respiratory Syndrome coronavirus (MERS-CoV). From the extracted time series, we estimated two summary statistics characterizing the long-term antibody response: the half-life of the long-lived component of the antibody response, and the percentage reduction in antibody response after one year. The half-life of the long-lived component of the antibody response was estimated by fitting a linear regression model to measurements of (log) antibody response taken greater than six months after symptom onset. The percentage reduction in antibody response after one year was estimated based on the reduction from the peak measured antibody response to the estimated antibody level at one year. Although a wide range of assays from ELISA to micro-neutrilisation were used in the reviewed studies, in this simple and approximate analysis we did not attempt to account for assay dependent effects, except to subtract background antibody levels where necessary.

Based on the estimated summary statistics, we assume that the long-term IgG antibody kinetics can be characterized as having a half-life of $d_l$ = 400 days with a 60% reduction after one year. In terms of the parameters of the mathematical model of antibody kinetics, this corresponds to prior estimates of $c_l = \log(2)/d_l = 0.0017$ and $\rho \sim 0.9$. For sensitivity analyses, we also considered scenarios where $d_l$ = 200 days and $d_l$ = 800 days.

For IgM antibody kinetics, we assumed $d_l$ = 100 days and $\rho \sim 0.9$. For sensitivity analyses, we also considered scenarios where $d_l$ = 50 days and $d_l$ = 200 days.

medRxiv preprint doi: https://doi.org/10.1101/2020.05.07.20093963.this version posted May 11, 2020. The copyright holder for this preprint (which was not certified by peer review) is the author/funder, who has granted medRxiv a license to display the preprint in perpetuity. It is made available under a CC-BY-NC-ND 4.0 International license .

**Table S1: Prior data on the duration of antibody responses to coronaviruses.** Data from longitudinal studies on measured antibody levels to SARS coronavirus, seasonal coronavirus 229E, and MERS coronavirus. For each study, the time series describing the antibody kinetics was extracted. The half-life of the long-lived component of the antibody response was estimated using measurements of antibody response measured after 6 months from symptom onset – the subset of the data used for this calculation is indicated in bold below. The percentage reduction in antibodies after one year is estimated based on the reduction from the peak measured response to the estimate antibody level at year.

| **study** | | | | | | | | | | | | **half-life (days)** | **1 year reduction** |
|---|---|---|---|---|---|---|---|---|---|---|---|---|---|
| SARS-CoV; Wu *et al.* Emerg Inf Dis. 2007; 13(10) | | | | | | | | | | | | | |
| time (days) | 180 | 365 | 730 | 1095 | | | | | | | | | |
| IgG | **0.96** | **0.638** | **0.516** | **0.249** | | | | | | | | 510 | |
| SARS-CoV; Mo *et al*. Respirology. 2006; 11: 49-53 | | | | | | | | | | | | | |
| time (days) | 7 | 15 | 30 | 60 | 90 | 180 | 270 | 360 | 450 | 540 | 720 | | |
| IgG | 0.01 | 1.86 | 2.36 | 2.83 | 2.81 | **2.73** | **2.38** | **1.91** | **1.42** | **1.00** | **0.80** | 181 | 60% |
| IgM | 0.01 | 1.13 | 1.80 | 1.30 | 0.69 | 0.06 | 0.01 | | | | | | 100% |
| Nab | 0.01 | 1.99 | 2.74 | 2.51 | 2.26 | **2.06** | **1.83** | **1.56** | **1.24** | **0.96** | **0.78** | 277 | 69% |
| SARS-CoV; Cao *et al.* NEJM. 2007; 357(11) | | | | | | | | | | | | | |
| time (days) | 30 | 120 | 210 | 300 | 480 | 720 | 900 | 1080 | | | | | |
| IgG | 196 | 244 | **114** | **112** | **64** | **36** | **33** | **28** | | | | 394 | 61% |
| Nab | 1034 | 1254 | **836** | **773** | **960** | **99** | **32** | **32** | | | | 154 | 33% |
| SARS-CoV; Liu *et al.* J Inf Dis. 2006. 193 | | | | | | | | | | | | | |
| time (days) | 30 | 120 | 210 | 300 | 480 | 720 | | | | | | | |
| IgG | 185 | 201 | **115** | **125** | **65** | **32** | | | | | | 254 | 49% |
| SARS-CoV; Tang *et al*. J Immunol. 2011; 186:7264-7268 | | | | | | | | | | | | | |
| time (days) | 24 | 120 | 210 | 300 | 480 | 720 | 900 | 1080 | 1600 | 2160 | | | |
| IgG | 305 | 252 | **128** | **170** | **66** | **31** | **36** | **33** | **6.9** | **6.0** | | 400 | 57% |
| seasonal coronavirus 229E; Callow *et al*. Epid. Inf. 1990; 105: 435-446 | | | | | | | | | | | | | |
| time (days) | 0 | 21 | 84 | 364 | | | | | | | | | |
| IgG | 2.45 | 3.18 | **2.62** | **2.51** | | | | | | | | 191 | 91% |
| IgA | 2.61 | 3.04 | **2.80** | **2.66** | | | | | | | | 150 | 87% |
| Nab | 1.43 | 9.84 | **5.46** | **2.19** | | | | | | | | 116 | 91% |
| MERS CoV; Choe *et al*. Emerg Inf Dis. 2017; 23(7) | | | | | | | | | | | | | |
| time (days) | 15 | 90 | 200 | 300 | 400 | | | | | | | | |
| IgG (S1) | 1.39 | 2.53 | **1.63** | **1.56** | **1.47** | | | | | | | 915 | 50% |

**Case study of early-stage SARS-Cov-2 antibody kinetics: hospitalized patients in Hong Kong**

We performed a secondary analysis of data from patients admitted to Princess Margaret Hospital and Queen Mary Hospital in Hong Kong, following the primary analysis by To, Tsang *et al* [1]. 23 patients with RT-qPCR confirmed SARS-CoV-2 infection were followed longitudinally for up to four weeks after initial onset of symptoms. Ten patients had severe COVID-19, all of whom required oxygen supplementation, and 13 patients had mild disease.

The Hong Kong based team expressed and purified recombinant proteins for receptor-binding domain (RBD) and nucleoprotein (NP). Genes encoding the spike RBD (amino acid residues 306 to 543 of the spike protein) and full length NP of SARS-CoV-2 were codon-optimized, synthesized and cloned. IgG and IgM antibody responses were quantified via

medRxiv preprint doi: https://doi.org/10.1101/2020.05.07.20093963.this version posted May 11, 2020. The copyright holder for this preprint (which was not certified by peer review) is the author/funder, who has granted medRxiv a license to display the preprint in perpetuity. It is made available under a CC-BY-NC-ND 4.0 International license .

the optical density (OD) from an enzyme immunoassay (EIA). Serial dilutions from 1:100 to 1:16,000 of a positive control serum were assayed for IgG responses. This allowed conversion of IgG antibody responses measured by EIA OD to dilutions. To determine the sero-positivity cutoff, the mean value of 93 anonymous archived serum specimens from 2018 plus 3 standard deviations was used. The cutoff values were: anti-NP IgG = 0.523 OD; anti-RBD IgG = 0.108 OD; anti-NP IgM = 0.177 OD; and anti-RBD IgM = 0.085. After conversion of the EIA OD values to dilutions, the sero-positivity cutoffs for IgG antibody responses were anti-NP IgG = 0.00682; and anti-RBD IgG = 0.002665.

**Results**

Estimated model parameters are presented in Table S2. Figure S1 provides an overview of the fitted antibody kinetics to all participants. Detailed individual-level fits to the data, with quantification of uncertainty are shown in Figures S2-S5. Comparing the early kinetics of the IgG and IgM response, we estimate that the time to anti-NP IgG sero-conversion was 11.0 days (inter-quartile range (IQR): 8.1, 11.6), and the time to anti-NP IgM sero-conversion was 11.9 days (IQR: 8.4, 15.8). The time to anti-RBD IgG sero-conversion was 8.6 days (IQR: 5.3, 10.4), and the time to anti-NP IgM sero-conversion was 11.6 days (IQR: 9.2, 28.6). Although time to sero-conversion is dependent on the selection of sero-positivity cutoff, this suggests that IgM responses are not induced before IgG responses, and that both are generated at approximately the same time.

medRxiv preprint doi: https://doi.org/10.1101/2020.05.07.20093963.this version posted May 11, 2020. The copyright holder for this preprint (which was not certified by peer review) is the author/funder, who has granted medRxiv a license to display the preprint in perpetuity. It is made available under a CC-BY-NC-ND 4.0 International license .

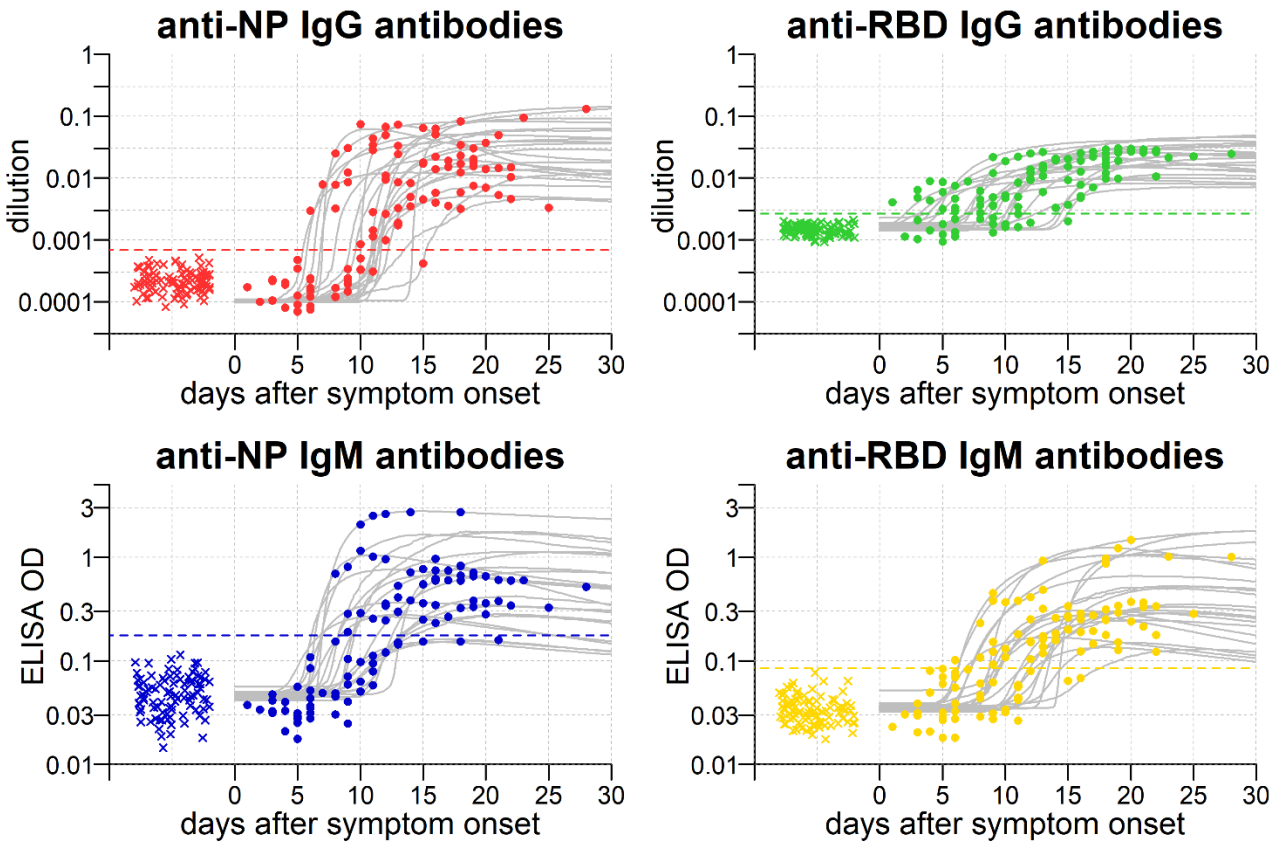


**Figure S1: SARS-CoV-2 antibody kinetics in Hong Kong patients.** Anti-nucleoprotein (NP) and anti-receptor-binding domain (RBD) antibody responses in 22 patients with PCR confirmed SARS-CoV-2 infection admitted to hospitals in Hong Kong. Measured antibody levels in patients are depicted as points. Measured antibody levels in negative controls are depicted as crosses. Grey lines show posterior median model prediction. The uncertainty of the model predictions is presented via 95% credible intervals in Figures S2-5. The horizontal dashed line represents the cutoff for sero-positivity.

medRxiv preprint doi: https://doi.org/10.1101/2020.05.07.20093963.this version posted May 11, 2020. The copyright holder for this preprint (which was not certified by peer review) is the author/funder, who has granted medRxiv a license to display the preprint in perpetuity. It is made available under a CC-BY-NC-ND 4.0 International license .

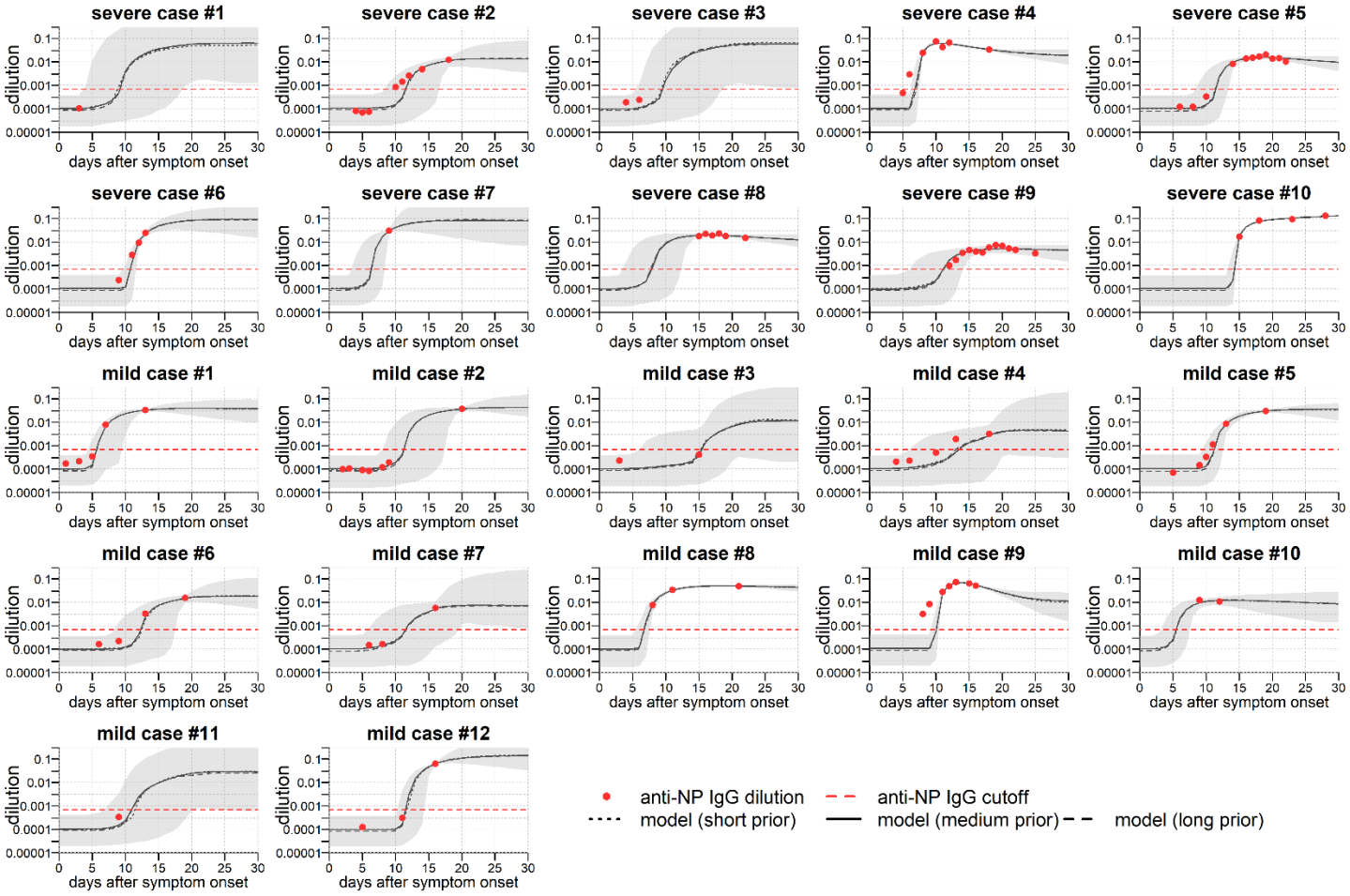


**Figure S2: Model fit to short-term data on anti-NP IgG antibody responses.** Measured antibody responses are shown as red points. Posterior median model predictions are shown as black lines, with 95% credible intervals in grey. The horizontal dashed line represents the cutoff for sero-positivity. Note that as there is no data on the long-term antibody response to SARS-CoV-2, three different sources of prior information were utilized. The half-life of the long-lived component of the antibody responses was assumed to be 200 days (short prior), 400 days (medium prior), or 800 days (long prior). Note that each of the three assumptions give near identical fits for the short-term kinetics displayed here.

medRxiv preprint doi: https://doi.org/10.1101/2020.05.07.20093963.this version posted May 11, 2020. The copyright holder for this preprint (which was not certified by peer review) is the author/funder, who has granted medRxiv a license to display the preprint in perpetuity. It is made available under a CC-BY-NC-ND 4.0 International license .

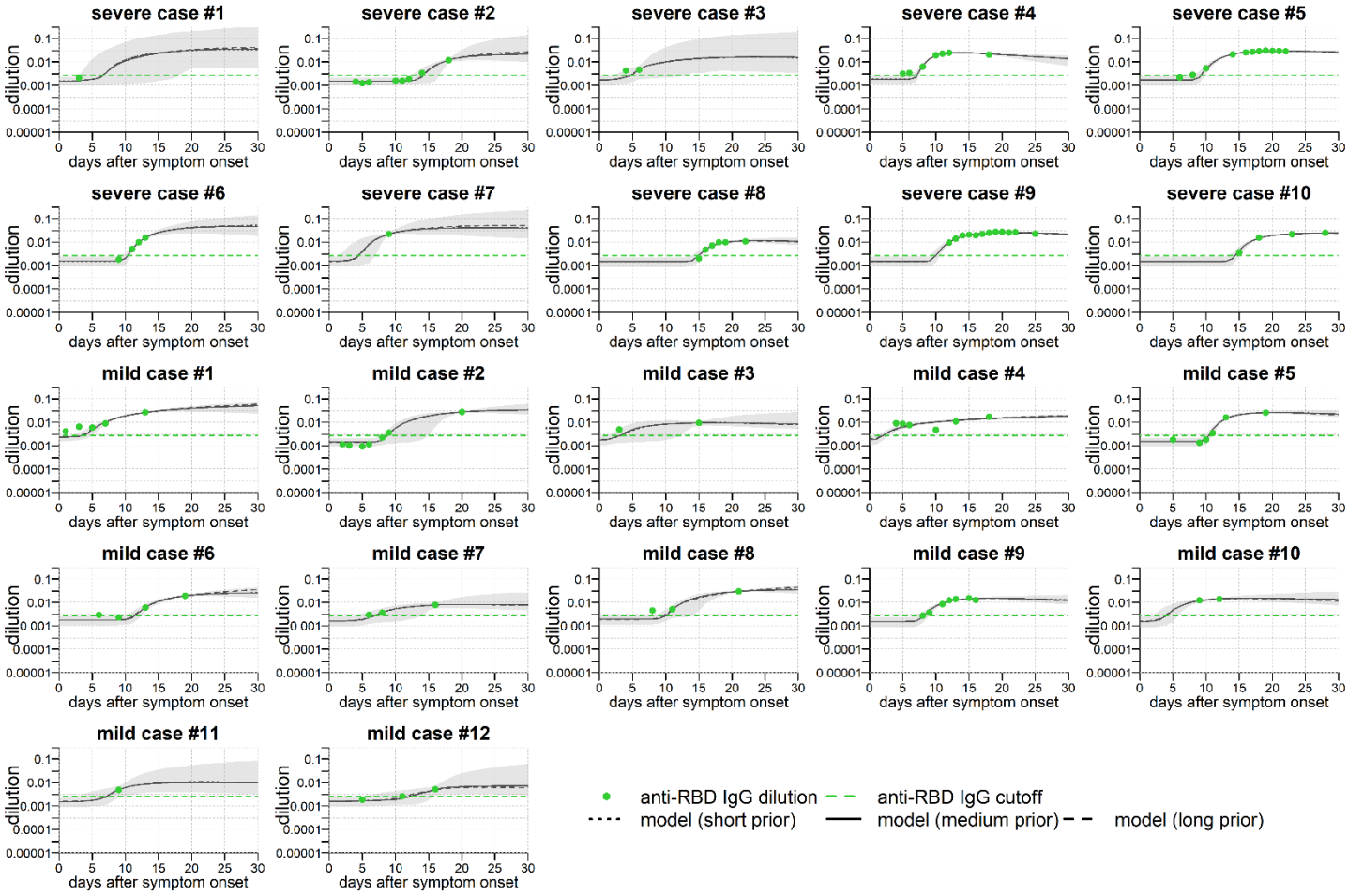


**Figure S3: Model fit to short-term data on anti-RBD IgG antibody responses.** Measured antibody responses are shown as red points. Posterior median model predictions are shown as black lines, with 95% credible intervals in grey. The horizontal dashed line represents the cutoff for sero-positivity. Note that as there is no data on the long-term antibody response to SARS-CoV-2, three different sources of prior information were utilized. The half-life of the long-lived component of the antibody responses was assumed to be 200 days (short prior), 400 days (medium prior), or 800 days (long prior). Note that each of the three assumptions give near identical fits for the short-term kinetics displayed here.

medRxiv preprint doi: https://doi.org/10.1101/2020.05.07.20093963.this version posted May 11, 2020. The copyright holder for this preprint (which was not certified by peer review) is the author/funder, who has granted medRxiv a license to display the preprint in perpetuity. It is made available under a CC-BY-NC-ND 4.0 International license .

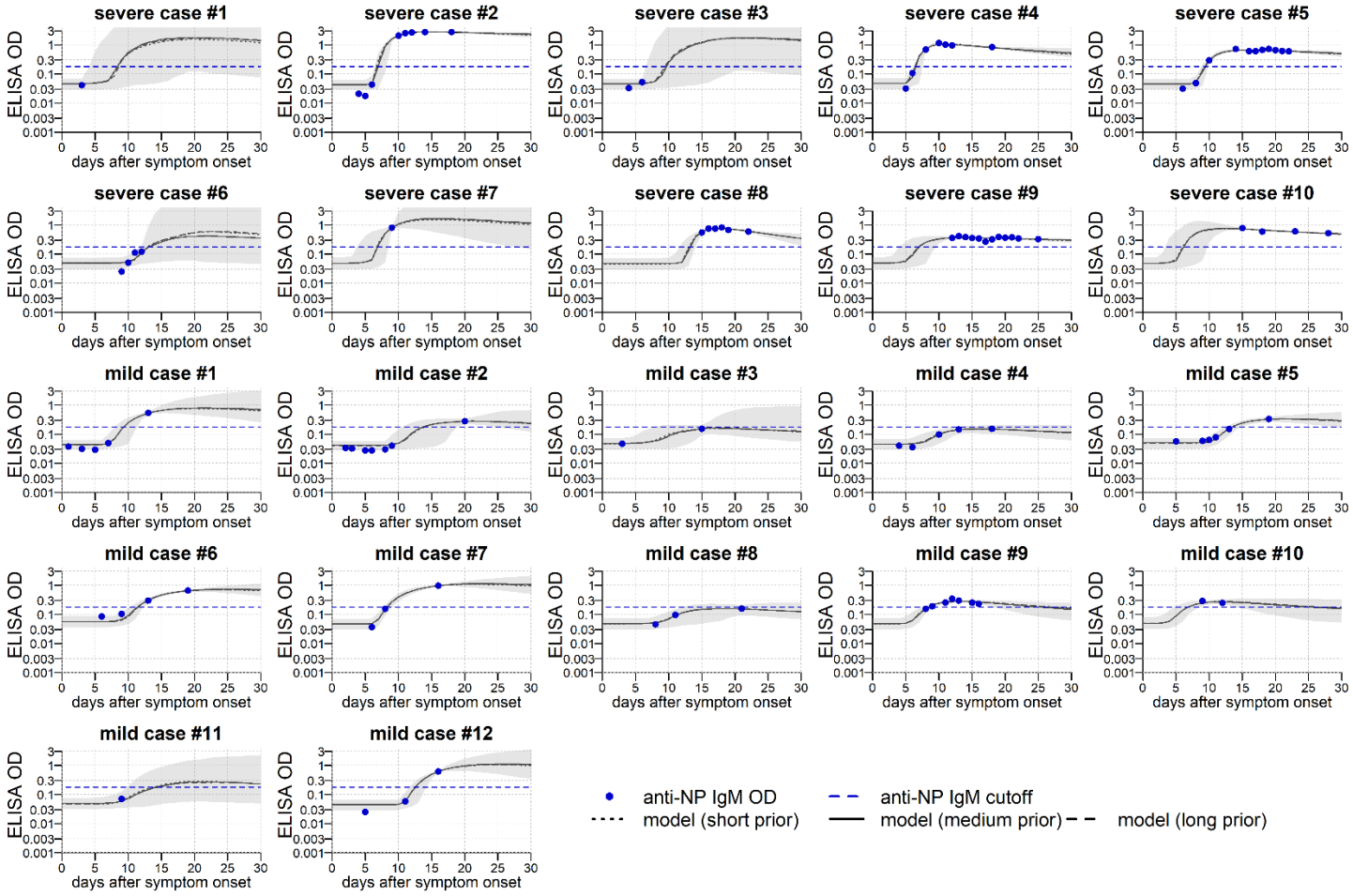


**Figure S4: Model fit to short-term data on anti-NP IgM antibody responses.** Measured antibody responses are shown as red points. Posterior median model predictions are shown as black lines, with 95% credible intervals in grey. The horizontal dashed line represents the cutoff for sero-positivity. Note that as there is no data on the long-term antibody response to SARS-CoV-2, three different sources of prior information were utilized. The half-life of the long-lived component of the antibody responses was assumed to be 50 days (short prior), 100 days (medium prior), or 200 days (long prior). Note that each of the three assumptions give near identical fits for the short-term kinetics displayed here.

medRxiv preprint doi: https://doi.org/10.1101/2020.05.07.20093963.this version posted May 11, 2020. The copyright holder for this preprint (which was not certified by peer review) is the author/funder, who has granted medRxiv a license to display the preprint in perpetuity. It is made available under a CC-BY-NC-ND 4.0 International license .

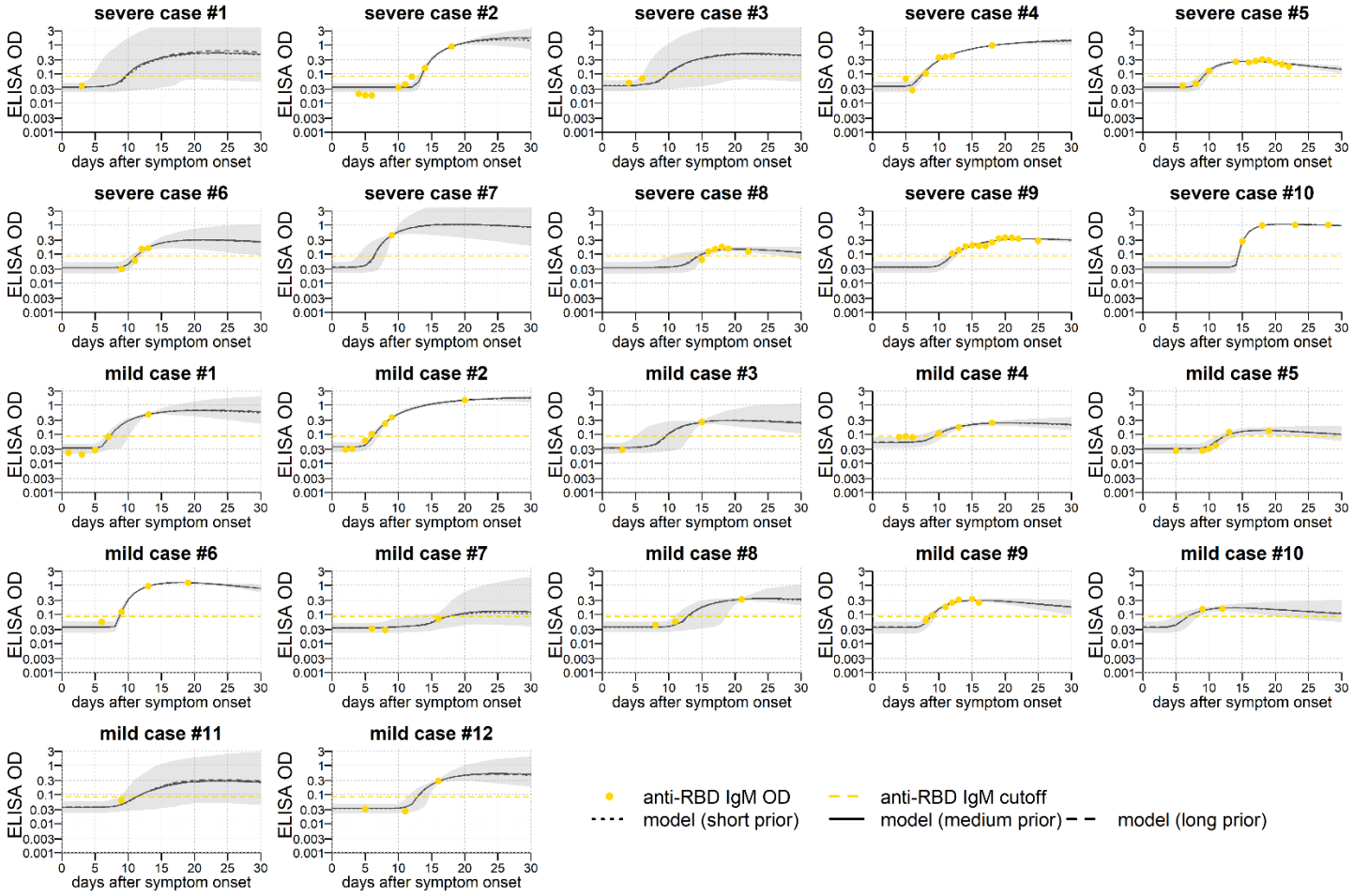


**Figure S5: Model fit to short-term data on anti-RBD IgM antibody responses.** Measured antibody responses are shown as red points. Posterior median model predictions are shown as black lines, with 95% credible intervals in grey. The horizontal dashed line represents the cutoff for sero-positivity. Note that as there is no data on the long-term antibody response to SARS-CoV-2, three different sources of prior information were utilized. The half-life of the long-lived component of the antibody responses was assumed to be 50 days (short prior), 100 days (medium prior), or 200 days (long prior). Note that each of the three assumptions give near identical fits for the short-term kinetics displayed here.

medRxiv preprint doi: https://doi.org/10.1101/2020.05.07.20093963.this version posted May 11, 2020. The copyright holder for this preprint (which was not certified by peer review) is the author/funder, who has granted medRxiv a license to display the preprint in perpetuity. It is made available under a CC-BY-NC-ND 4.0 International license .

**Table S2: Parameter estimates for antibody kinetics model fitted to Hong Kong data.** Parameters of the antibody kinetics model are presented as posterior medians with 95% credible intervals. The model is fitted in a mixed-effects framework, so for every parameter we estimate the distribution within the entire population rather than a fixed value. We present the mean and standard deviation as summary statistics for the estimated distributions

| description | parameter | prior | NP IgG | RBD IgG | NP IgM | RBD IgM |
|---|---|---|---|---|---|---|
| *mean of population-level distribution* | | | | | | |
| background IgG level | $A_{bg}$ | 0.001 (1.1x10$^{-6}$, 1.1) | 0.00011 (2.6x10$^{-5}$, 0.0003) | 0.0015 (0.0013, 0.0017) | – | – |
| background IgM level | $A_{bg}$ | 0.03 (0.001, 1.0) | – | – | 0.049 (0.043, 0.054) | 0.036 (0.032, 0.04) |
| ASC boost in mild cases (IgG) | $\beta_{mild}$ | 0.01 (0.0001, 1.2) | 0.014 (0.006, 0.051) | 0.0028 (0.0015, 0.0053) | – | – |
| ASC boost in mild cases (IgM) | $\beta_{mild}$ | 0.11 (0.01, 1.2) | – | – | 0.085 (0.048, 0.17) | 0.08 (0.04, 0.16) |
| ASC boost in severe cases (IgG) | $\beta_{sev}$ | 0.01 (0.0001, 1.2) | 0.028 (0.01, 0.207) | 0.0056 (0.0034, 0.0099) | – | – |
| ASC boost in severe cases (IgM) | $\beta_{sev}$ | 0.11 (0.01, 1.2) | – | – | 0.67 (0.29, 2.8) | 0.14 (0.07, 0.46) |
| delay in generation of antibody response (days) | $\tau$ | 5.4 (2.5, 15.1) | 9.6 (7.7, 11.9) | 7.8 (5.6, 11.7) | 7.9 (6.4, 9.8) | 8.7 (7.0, 10.7) |
| half-life of memory cells (days) | $d_m$ | 2.1 (1.5, 4.0) | 2.0 (1.3, 7.8) | 1.8 (1.3, 2.8) | 2.0 (1.3, 5.7) | 2.2 (1.5, 4.9) |
| half-life of short-lived ASCs (days) | $d_s$ | 3.2 (1.9, 9.2) | 2.5 (1.8, 4.1) | 2.4 (1.8, 3.7) | 2.4 (1.7, 3.8) | 2.8 (2.0, 4.7) |
| half-life of long-lived ASCs (days) (IgG) | $d_l$ | 400 (302, 567) | 408 (227, 727) | 417 (230, 771) | – | – |
| half-life of long-lived ASCs (days) (IgM) | $d_l$ | 100 (76, 142) | – | – | 104 (68, 163) | 103 (66, 167) |
| half-life of IgG molecules (days) | $d_a$ | 21 (18·7, 24·1) | 43·5 (25·7, 243·6) | 21·3 (18·4, 28·7) | – | – |
| half-life of IgM molecules (days) | $d_a$ | 10 (9.1, 11.5) | – | – | 10.8 (9.3, 164.2) | 10.2 (9.2, 13.2) |
| proportion of short-lived ASCs | $\rho$ | 90% (65%, 95%) | 90% (79%, 94%) | 80% (57%, 94%) | 93% (65%, 97%) | 89% (62%, 98%) |
| *standard deviation of population-level distribution* | | | | | | |
| background IgG level | $A_{bg}$ | 0.0006 (6x10$^{-7}$, 0.8) | 5.7x10$^{-5}$ (1.0x10$^{-5}$, 0.00013) | 0.0004 (0.0003, 0.0005) | – | – |
| background IgM level | $A_{bg}$ | 0.01 (0.0003, 0.5) | – | – | 0.01 (0.007, 0.015) | 0.008 (0.006, 0.011) |
| ASC boost in mild cases (IgG) | $\beta_{mild}$ | 0.006 (5.4x10$^{-5}$, 0.9) | 0.020 (0.006, 0.23) | 0.0017 (0.0007, 0.005) | – | – |
| ASC boost in mild cases (IgM) | $\beta_{mild}$ | 0.06 (0.004, 1.1) | – | – | 0.045 (0.020, 0.17) | 0.06 (0.03, 0.21) |
| ASC boost in severe cases (IgG) | $\beta_{sev}$ | 0.006 (5.4x10$^{-5}$, 0.9) | 0.048 (0.01, 2.0) | 0.0030 (0.0015, 0.008) | – | – |
| ASC boost in severe cases (IgM) | $\beta_{sev}$ | 0.06 (0.004, 1.1) | – | – | 0.55 (0.19, 4.9) | 0.17 (0.06, 1.4) |
| delay in generation of antibody response (days) | $\tau$ | 3.5 (1.2, 34.6) | 4.2 (2.8, 6.9) | 6.5 (3.8, 17.5) | 3.5 (2.3, 5.9) | 3.8 (2.6, 6.4) |
| half-life of memory cells (days) | $d_m$ | 1.1 (0.5, 7.2) | 1.8 (0.6, 35.3) | 1.0 (0.5, 3.5) | 1.8 (0.6, 18.5) | 1.8 (0.7, 11.87) |
| half-life of short-lived ASCs (days) | $d_s$ | 2.3 (0.9, 29.2) | 1.3 (0.6, 3.5) | 1.2 (0.6, 2.8) | 1.2 (0.6, 3.1) | 1.6 (0.7, 4.6) |
| half-life of long-lived ASCs (days) (IgG) | $d_l$ | 109 (56, 349) | 111 (47, 384) | 114 (47, 404) | – | – |

medRxiv preprint doi: https://doi.org/10.1101/2020.05.07.20093963.this version posted May 11, 2020. The copyright holder for this preprint (which was not certified by peer review) is the author/funder, who has granted medRxiv a license to display the preprint in perpetuity. It is made available under a CC-BY-NC-ND 4.0 International license .

| | | | | | | |
|---|---|---|---|---|---|---|
| half-life of long-lived ASCs (days) (IgM) | $d_l$ | 22 (10, 69) | – | – | 22 (11, 67) | 23 (11, 73) |
| half-life of IgG molecules (days) | $d_a$ | 3·2 (1·8, 8.6) | 84·0 (22, 2808) | 5·4 (2·0, 27) | – | – |
| half-life of IgM molecules (days) | $d_a$ | 2.2 (1.2, 6.2) | – | – | 4.4 (1.5, 2770) | 2.6 (1.3, 12) |
| proportion of short-lived ASCs | $\rho$ | 0.07 (0.02, 0.40) | 0.06 (0.02, 0.26) | 0.25 (0.04, 0.45) | 0.08 (0.02, 0.42) | 0.18 (0.02, 0.44) |
| *observational variance* | | | | | | |
| standard deviation for ELISA measurements (IgG) | $\sigma_{obs}$ | 0·004 (0·0002, 0·1) | 0·0026 (0·0023, 0·0030) | 0·0011 (0·0009, 0·0013) | – | – |
| standard deviation for ELISA measurements (IgM) | $\sigma_{obs}$ | 0·04 (0·002, 1) | – | – | 0·031 (0·025, 0.037) | 0·022 (0·019, 0.025) |

medRxiv preprint doi: https://doi.org/10.1101/2020.05.07.20093963.this version posted May 11, 2020. The copyright holder for this preprint (which was not certified by peer review) is the author/funder, who has granted medRxiv a license to display the preprint in perpetuity. It is made available under a CC-BY-NC-ND 4.0 International license .

**Table S3: Parameter estimates for antibody kinetics model fitted to France data.** Parameters of the antibody kinetics model are presented as posterior medians with 95% credible intervals. The model is fitted in a mixed-effects framework, so for every parameter we estimate the distribution within the entire population rather than a fixed value. We present the mean and standard deviation as summary statistics for the estimated distributions

| description | parameter | prior | $S^{tri}$ | RBD | S1 | S2 |
|---|---|---|---|---|---|---|
| *mean of population-level distribution* | | | | | | |
| background IgG level | $A_{bg}$ | 0.001 (1.1x10$^{-6}$, 1.1) | 7.8x10$^{-6}$ (6.5x10$^{-6}$, 9.6x10$^{-6}$) | 1.1x10$^{-5}$ (8.5x10$^{-6}$, 1.6x10$^{-5}$) | 2.1x10$^{-5}$ (1.4x10$^{-5}$, 3.1x10$^{-5}$) | 1.3x10$^{-5}$ (9.4x10$^{-6}$, 1.9x10$^{-5}$) |
| ASC boost | B | 0.01 (0.0001, 1.2) | 0.00023 (0.00016, 0.00035) | 0.00014 (9.0x10$^{-5}$, 0.0002) | 0.00032 (0.0002, 0.0006) | 0.0004 (0.0003, 0.0006) |
| delay in generation of antibody response (days) | τ | 5.4 (2.5, 15.1) | 4.8 (3.3, 6.0) | 4.4 (2.8, 5.8) | 4.6 (2.4, 6.1) | 5.7 (4.3, 6.8) |
| half-life of memory cells (days) | $d_m$ | 2.1 (1.5, 4.0) | 1.9 (1.5, 2.6) | 1.8 (1.5, 2.5) | 2.0 (1.5, 3.1) | 1.9 (1.5, 2.8) |
| half-life of short-lived ASCs (days) | $d_s$ | 3.2 (1.9, 9.2) | 3.0 (2.2, 4.4) | 3.0 (2.2, 4.2) | 3.0 (2.2, 4.3) | 3.0 (2.3, 4.3) |
| half-life of long-lived ASCs (days) | $d_l$ | 400 (302, 567) | 404 (239, 777) | 407 (227, 740) | 418 (231, 750) | 403 (234, 762) |
| half-life of IgG molecules (days) | $d_a$ | 21 (18·7, 24·1) | 21·1 (18·7, 23·9) | 21·2 (18·8, 23·4) | 21·2 (18·7, 23·9) | 21·1 (18·8, 23·9) |
| proportion of short-lived ASCs | $\rho$ | 90% (65%, 95%) | 81% (57%, 95%) | 81% (58%, 93%) | 84% (0%, 95%) | 76% (57%, 94%) |
| *standard deviation of population-level distribution* | | | | | | |
| background IgG level | $A_{bg}$ | 0.0006 (6x10$^{-7}$, 0.8) | 4.5x10$^{-6}$ (3.3x10$^{-6}$, 6.3x10$^{-6}$) | 8.0x10$^{-6}$ (5.1x10$^{-6}$, 1.3x10$^{-5}$) | 1.9x10$^{-5}$ (1.0x10$^{-5}$, 3.4x10$^{-5}$) | 1.0x10$^{-5}$ (6.0x10$^{-6}$, 1.8x10$^{-5}$) |
| ASC boost | β | 0.006 (5.4x10$^{-5}$, 0.9) | 0.0002 (0.0001, 0.0004) | 0.00011 (6.7x10$^{-5}$, 0.0002) | 0.00048 (0.00022, 0.0012) | 0.0004 (0.0002, 0.0008) |
| delay in generation of antibody response (days) | τ | 3.5 (1.2, 34.6) | 1.4 (1.0, 1.8) | 1.3 (0.9, 1.9) | 1.4 (0.8, 2.0) | 1.9 (1.4, 2.7) |
| half-life of memory cells (days) | $d_m$ | 1.1 (0.5, 7.2) | 1.3 (0.7, 3.1) | 1.2 (0.7, 2.7) | 1.7 (0.8, 5.4) | 1.4 (0.7, 3.9) |
| half-life of short-lived ASCs (days) | $d_s$ | 2.3 (0.9, 29.2) | 1.1 (0.6, 2.1) | 1.1 (0.6, 2.1) | 1.1 (0.6, 2.1) | 1.1 (0.6, 2.1) |
| half-life of long-lived ASCs (days) | $d_l$ | 109 (56, 349) | 110 (48, 378) | 112 (47, 408) | 113 (46, 403) | 112 (48, 372) |
| half-life of IgG molecules (days) | $d_a$ | 3·2 (1·8, 8.6) | 3·2 (1.8, 7) | 3·3 (1·8, 7) | 3·3 (1.8, 7.2) | 3·3 (1·8, 7.3) |
| proportion of short-lived ASCs | $\rho$ | 0.07 (0.02, 0.40) | 0.19 (0.008, 0.45) | 0.19 (0.008, 0.45) | 0.0076 (1.0x10$^{-11}$, 0.44) | 0.28 (0.02, 0.45) |
| *observational variance* | | | | | | |
| log scale standard deviation for Luminex measurements | $\sigma_{obs}$ | 0·71 (0·18, 2.75) | 0·92 (0·84, 1.0) | 1·40 (1·26, 1.54) | 1·08 (0·92, 1.25) | 1·15 (0·99, 1.29) |